J. Fluid Mech. (2023), *vol*. 973, A30, doi:10.1017/jfm.2023.769

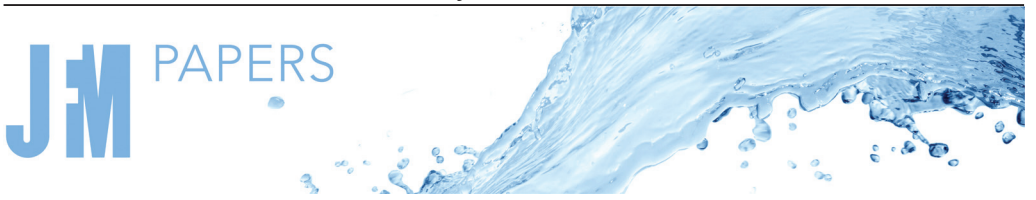

Taylor columns and inertial-like waves in a three-dimensional odd viscous liquid

E. Kirkinis[1,2,†] **and M. Olvera de la Cruz**[1,2]

[1]Department of Materials Science & Engineering, Robert R. McCormick School of Engineering and Applied Science, Northwestern University, Evanston, IL 60208, USA

[2]Center for Computation and Theory of Soft Materials, Northwestern University, Evanston, IL 60208, USA

(Received 29 March 2023; revised 16 August 2023; accepted 9 September 2023)

Odd viscous liquids are endowed with an intrinsic mechanism that tends to restore a displaced particle back to its original position. Since the odd viscous stress does not dissipate energy, inertial oscillations and inertial-like waves can become prominent in such a liquid. In this paper, we show that an odd viscous liquid in three dimensions may give rise to such axially symmetric waves and also to plane-polarized waves. We assume tacitly that an anisotropy axis giving rise to odd viscous effects has already been established, and proceed to investigate the effects of odd viscosity on fluid flow behaviour. Numerical simulations of the full Navier–Stokes equations show the existence of inertial-like waves downstream of a body that moves slowly along the axis of an odd viscous liquid filled cylinder. The wavelength of the numerically determined oscillations agrees well with the developed theoretical framework. When odd viscosity is the dominant effect in steady motions, a modified Taylor–Proudman theorem leads to the existence of Taylor columns inside such a liquid. Formation of the Taylor column can be understood as a consequence of helicity segregation and energy transfer along the cylinder axis at group velocity, by the accompanying inertial-like waves, whenever the reflection symmetry of the system is lost. A number of Taylor column characteristics known from rigidly rotating liquids are recovered here for a non-rotating odd viscous liquid. These include counter-rotating swirling liquid flow above and below a body moving slowly along the anisotropy axis. Thus in steady motions, odd viscosity acts to suppress variations of liquid velocity in a direction parallel to the anisotropy axis, inhibiting vortex stretching and vortex twisting. In unsteady and nonlinear motions, odd viscosity enhances the vorticity along the same axis, thus affecting both vortex stretching and vortex twisting.

Key words: waves in rotating fluids

† Email address for correspondence: ekirkinis@gmail.com

1. Introduction

Avron, Seiler & Zograf (1995) showed that the viscosity tensor $\eta_{\alpha\beta\gamma\delta}$ of the Cauchy stress of a classical liquid,

$$\sigma_{\alpha\beta} = \eta_{\alpha\beta\gamma\delta} V_{\gamma\delta}, \tag{1.1}$$

can be decomposed into a symmetric part and an antisymmetric part, i.e. $\eta_{\alpha\beta\gamma\delta} = \eta^S_{\alpha\beta\gamma\delta} + \eta^A_{\alpha\beta\gamma\delta}$, where

$$\eta^S_{\alpha\beta\gamma\delta} = \eta^S_{\gamma\delta\alpha\beta} \quad \text{and} \quad \eta^A_{\alpha\beta\gamma\delta} = -\eta^A_{\gamma\delta\alpha\beta}. \tag{1.2a,b}$$

Here, $V_{\gamma\delta} = (\partial u_\gamma/\partial x_\delta + \partial u_\delta/\partial x_\gamma)/2$ is the rate-of-strain tensor, and u_α is the liquid velocity. The stress tensor (1.1) based on η^S is dissipative. It results in viscous heating (Landau & Lifshitz 1987, § 49) which is a positive-definite quadratic form $\mathrm{tr}(\sigma V) = V_{\alpha\beta}\eta^S_{\alpha\beta\gamma\delta}V_{\gamma\delta} > 0$. Here, η^A does not contribute to viscous heating due to its antisymmetry between the first and second pairs of indices.

The non-dissipative stress $\eta^A_{\alpha\beta\gamma\delta}V_{\gamma\delta}$ is called the odd viscous (or anomalous) stress tensor, and its accompanying coefficients are called odd or Hall viscosity coefficients. This type of behaviour can be induced, for instance, by a magnetic field, giving rise to an anisotropy axis along its direction. Avron *et al.* (1995) provided a clear physical interpretation of the odd stress tensor that carries over to classical systems. Compression or dilatation gives rise to shear, and vice versa. Thus it is easy to show, for instance, that a cylinder rotating about its axis in an odd viscous liquid gives rise to a stress $\sigma^o_{rr} = 2\eta_o\Omega$ directed normal to the cylinder surface (Avron 1998; Kirkinis 2023), where η_o is the dynamic coefficient of odd viscosity, and Ω is the constant angular velocity of the cylinder.

The ramifications of odd viscosity in classical mechanical systems have been investigated only in the recent literature. Noteworthy are experiments showing blobs of a liquid composed of micron-size spinning magnets whose surface undulations were attenuated by a shear-stress-induced odd normal stress. (The shear stress is generated by the collective rotation of the particles close to the free surface; cf. Soni *et al.* 2019.) In three dimensions, Khain *et al.* (2022) showed that odd viscous liquids, in the absence of inertia, give rise to unconventional fluid flow behaviour such as the stabilization of a sedimenting cloud of particles due to an odd-viscosity-induced azimuthal velocity field generated by the gravitational stretching of the cloud in the axial direction, in agreement with the physical interpretation of Avron *et al.* (1995). In two dimensions, such an odd-viscosity-induced azimuthal component can be seen in the radial expansion of a bubble (Ganeshan & Abanov 2017). From a microscopic point of view, the mechanisms that may give rise to an odd viscosity coefficient include broken parity, broken time reversal and microscopic torques. The latter can be traced back to the literature of liquids endowed with rotational degrees of freedom (Dahler & Scriven 1961), which have been employed in the continuum description of magnetic liquids (Rinaldi 2002; Kirkinis 2017). Other odd-viscosity-induced phenomena have been collected succinctly in the recent review by Fruchart, Scheibner & Vitelli (2023, figure 1).

The stabilizing behaviour induced by odd viscosity in Soni *et al.* (2019), as well as in other works that have appeared in the recent literature (see e.g. Kirkinis & Andreev 2019), implies that the odd viscous stress may endow its medium with an intrinsic restoring property. Since the odd viscous stress does not dissipate energy, an excitation given to the fluid may establish an oscillation. Such an oscillation may further initiate wave propagation and periodic expansion and contraction in a plane perpendicular to the propagation direction. This type of motion (in a non-odd viscous liquid) is called an inertial wave and is present in the ocean, driving its upper mixing (Asselin & Young 2020),

constituting half of its energy and being responsible for the majority of its vertical shear. Inertial waves also appear in the celestial sphere (Ogilvie 2013) and in the technology of propulsion (Gao *et al.* 2020). It has also been argued that inertial waves in the Earth's interior are associated with a dynamo dipole and with helicity segregation (Davidson 2014; Davidson & Ranjan 2018). Waves in odd viscous liquids have been investigated on a number of occasions. These include gravity waves (Abanov, Can & Ganeshan 2018) in incompressible liquids, shock waves (Banerjee *et al.* 2017) and three-dimensional waves in active matter (Markovich & Lubensky 2021).

A three-dimensional odd viscous liquid may also give rise to Taylor columns. Taylor columns are known to form when bodies move slowly in (non-odd viscous) rapidly rotating liquids (Davidson 2013). For instance, a slowly moving body along the axis of a rigidly rotating liquid gives rise to a flow whose component along the axis of rotation can decouple from its lateral plane counterpart. (By lateral plane, we will mean the plane whose normal is the anisotropy axis.) Thus a Taylor column will form whose speed will be identical to the speed of the slowly moving body that it circumscribes. There are certain restrictive conditions that need to be satisfied in order for a Taylor column to form. These are the small Rossby and Ekman numbers as defined in (B1*a*,*b*), which thus require high angular velocity of rotation (and slow motions in the rotating frame) and low values of the shear viscosity coefficient. Taylor columns are present in a multitude of diverse areas: cold water and low salinity domes form over seamounts (e.g. the Rockall, Faroe and Hutton Banks) of high chlorophyll and nutrient levels, enabling larval diversity hotspots (Dransfeld, Dwane & Zuur 2009) by entrapping plankton (presumably by entraining matter through Stewartson layers). A turbulent ocean below the icy crust of Enceladus and Europa is likely to transfer energy through counter-rotating zonal jets inside a Taylor column (Bire *et al.* 2022).

Taylor columns form in (non-odd viscous) rotating liquids because the Coriolis force is always perpendicular to the velocity field (the latter expressed in the frame of reference rotating with the liquid). Thus a radial motion of a fluid particle gives rise to a commensurate azimuthal component, and vice versa. This is reminiscent of the physical interpretation given by Avron *et al.* (1995) to odd viscosity, and thus leads to the possibility of observing Taylor columns in such a liquid. As is the case in their rigidly rotating counterparts, Taylor columns in (non-rotating) odd viscous liquids can be observed when certain restrictions are satisfied. These correspond to the smallness of the parameter $\mathcal{M}^{-1} = aU/\nu_0$, which requires a large coefficient of kinematic odd viscosity ν_o and slow motions. (Here, U can be understood as the velocity of a body moving slowly in an odd viscous liquid, and a is a characteristic length scale.) In addition, the effect of shear viscosity ν_e should be small, and so should be the Ekman number $\mathcal{T}^{-1} = \nu_e/\nu_o$; see (6.2*a*,*b*).

Questions may arise as to whether this type of behaviour in three-dimensional odd viscous liquids will ever be observed in a laboratory setting. Both odd viscosity coefficients (termed η_o and η_4 here) were measured in a series of experiments of pressure-driven gas flow under a magnetic field by Beenaker and coworkers (Hulsman *et al.* 1970) (termed η_4 and η_5 in this reference, respectively). In these experiments, pressure-driven flow of one of the gases N_2, CO, CH_4 and HD, in a channel of rectangular cross-section, met two small holes located at opposite sides in the narrow sides of the channel and connected with a differential manometer. When a magnetic field was applied, a pressure gradient was generated along the line connecting the holes, transverse to the flow direction. The resulting pressure difference $p_A - p_B$ over the channel width

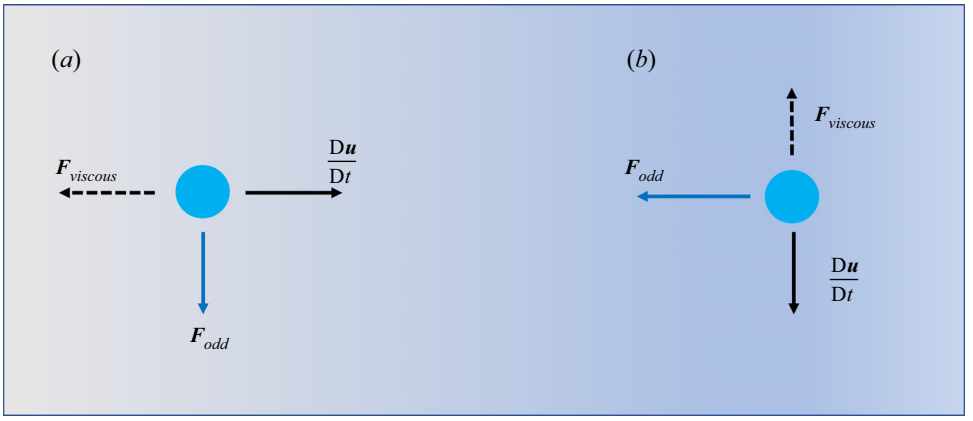

Figure 1. Restoring mechanism associated with odd viscosity in two dimensions. (*a*) Acceleration of a fluid particle is resisted by the viscous force; its odd viscous counterpart acts perpendicularly to the axis of the viscous force. (*b*) The new tangential motion acquired by the fluid particle is resisted by the viscous force, thus a new odd viscous force acts perpendicularly. The direction of the latter is opposite to the original fluid particle acceleration.

was measured with the differential manometer, and the data were analysed with the same set of equations that we employ in the present paper. The physical mechanism of coupling between the magnetic field and the molecule magnetic moment is discussed in detail by Lifshitz & Pitaevskii (1981, § 13). It is likewise expected that measurements of three-dimensional odd viscous coefficients will be undertaken in a liquid, although it is not clear at this moment in time what the nature of this liquid will be.

In figure 1, we demonstrate schematically the restoring property induced by odd viscosity on a two-dimensional liquid. In three dimensions, when odd viscosity dominates over its shear counterpart, the restoring behaviour can be established qualitatively by balancing the inertial terms in the Navier–Stokes equations with the odd viscous term (cf. Tritton (1988, § 16.6) for the case of a rotating liquid). Let $v > 0$ be the velocity of an isolated unit mass fluid particle in a plane perpendicular to the anisotropy axis (say, in the azimuthal direction). Balance between inertia and odd viscous terms leads to

$$\frac{v^2}{r} = \nu_o \frac{v}{r^2}, \tag{1.3}$$

giving $v = \nu_o/r$, where $\nu_o = \eta_o/\rho > 0$ is the odd kinematic coefficient of viscosity. Thus the particle will move in circles of radius $r = \nu_o/v$. The period T_o of this rotation depends on the distance from the axis of anisotropy, i.e. $T_o = 2\pi r^2/\nu_o$, and this shows that an odd viscous liquid is endowed with an intrinsic frequency

$$\omega_o = \frac{\nu_o}{r^2}. \tag{1.4}$$

Although the above argument is only schematic, the derived expression for the frequency ω_o is recovered in the following quantitative analysis (see (3.17)), at least in the short wavelength limit. A more satisfying argument supporting the restoring effect of odd viscous liquids is relegated to the end of § 3.1.

In a three-dimensional odd viscous liquid, we observe waves whose motion resembles the inertial waves occurring in (non-odd viscous) rigidly rotating liquids. The anisotropy axis inherent in the odd stress plays the role of the rotating axis of a rigidly rotating liquid.

When the inertial-like waves induced by odd viscosity are plane-polarized, there is a superposition of two oppositely directed waves; particle paths are helical, and this is reflected in the sign of the helicity density (vorticity times velocity) associated with each direction. When the propagation direction is at right angles to the odd anisotropy axis, the phase velocity vanishes and the system suffers a loss of reflection symmetry (Moffatt 1970). Energy then propagates along the anisotropy axis at maximum group velocity and is accompanied by helicity of a commensurate sign. This effect is called 'segregation of helicity' in (non-odd viscous) rigidly rotating liquids (Davidson & Ranjan 2018) and is believed to be important in understanding the dipolar nature of planetary dynamos since in a planet, mean helicity is segregated spatially, having opposite signs at the northern and southern hemispheres, respectively.

In this paper, we will assume tacitly that such an axis of anisotropy has already been established, and proceed by examining the consequences of the resulting odd viscous stress to fluid motions. Here, we consider fluid motions in a three-dimensional odd viscous liquid. The paper proceeds in the following manner. In § 2, we describe the constitutive law for the odd viscous liquid that will give rise to the inertial-like waves (Lifshitz & Pitaevskii 1981, § 13). Section 3.1 establishes the existence of the inertial-like waves in an odd viscous liquid. These are waves that propagate along the axis of anisotropy and wrapped in coaxial cylinders where liquid does not cross. We determine theoretically the frequency and wavelength of propagated modes. We provide a more satisfying, yet still qualitative discussion of the 'elasticity' of an odd viscous liquid. In § 3.4, we solve numerically the full Navier–Stokes equations for the slow motion of a sphere inside an odd viscous liquid. Such motions generate liquid oscillations downstream the body. Their wavelength is in astonishing agreement with the theoretical value obtained from the inertial theory of § 3.1. In § 3.5, we establish the existence of inertial-like waves exterior to a cylinder and extending to infinity. In § 3.6, we derive the frequency, phase and group velocities of three-dimensional plane-polarized waves. These differ from their axisymmetric counterparts derived in § 3.1, which also vary in the propagation direction. They are also special as they segregate helicity, and this is discussed in § 4. In § 5, we derive a modified Taylor–Proudman theorem. This means that when odd viscosity dominates over shear viscosity and inertial terms, the motion in the lateral plane becomes decoupled to the motion of the fluid along the anisotropy axis. This opens up the prospect of existence of Taylor columns in odd viscous liquids, which we explore in § 6. Since the study of Taylor columns entails overwhelming details, in order to provide some structure in our discussion we follow the map set up by Maxworthy (1970) for the slow motion of a particle. We thus solve numerically the Navier–Stokes equations, and find many similarities to Maxworthy's work: counter-rotating swirling motion above and below the sphere, a forward and a rearward 'slug', a stagnant region, indication of an Ekman layer surrounding the sphere, etc.

In § 8, we revisit the foregoing results by introducing another part of the odd stress tensor (the η_4 part of the stress in the notation followed by Lifshitz & Pitaevskii 1981, §§ 13 and 58). This provides a complete picture of odd viscous effects that may be present in a liquid. A consequence of including both viscosity coefficients is the more diverse behaviour displayed by the velocity field (it can now resemble Kelvin functions). Helicity is still conserved in such a composite liquid when its velocity field is determined by plane-polarized waves.

The problems that we discuss in this paper present many similarities to flows generated in a rotating liquid and described in a rotating frame of reference. Thus, throughout the paper, where appropriate, we establish connections to these effects. We conclude in

Appendix B by outlining a few facts about rotating fluids that are of relevance to this paper (although this paper is not about rotating liquids).

2. Constitutive relations of a three-dimensional odd viscous liquid

In fluid mechanics, the constitutive law (the Cauchy stress tensor) of a Newtonian liquid is usually introduced following the phenomenological approach (cf. Batchelor 1967, § 3.3) or more rigorously by employing the principle of objectivity (cf. Truesdell & Noll 1992). It is, however, possible to also introduce the notion of stress through the Onsager principle of the symmetry of the kinetic coefficients (Lifshitz & Pitaevskii 1981, § 13). When these coefficients (here, the viscosity tensor $\eta_{\alpha\beta\gamma\delta}$ that we introduced in (1.1)) depend on external fields, say $\boldsymbol{B}$, in the direction $\boldsymbol{b} = \boldsymbol{B}/B$, that change sign under time reversal, the symmetry of the kinetic coefficients is ensured when

$$\eta_{\alpha\beta\gamma\delta}(\boldsymbol{b}) = \eta_{\gamma\delta\alpha\beta}(-\boldsymbol{b}). \tag{2.1}$$

For an incompressible liquid, the stress tensor (1.1), subject to such a field, obtains the form

$$\begin{aligned}\sigma'_{\alpha\beta} = {} & 2V_{\alpha\beta}(\eta+\eta_1) + V_{\beta\gamma}\left[2(\eta_2-\eta_1)b_\gamma b_\alpha + \eta_3 b_{\alpha\gamma}\right] \\ & + V_{\alpha\gamma}\left[2(\eta_2-\eta_1)b_\gamma b_\beta + \eta_3 b_{\beta\gamma}\right] \\ & + V_{\gamma\delta}\left[(\eta_1+\zeta_1)\delta_{\alpha\beta}b_\gamma b_\delta + (\eta_1-4\eta_2)b_\alpha b_\beta b_\gamma b_\delta\right. \\ & \left. + (2\eta_4-\eta_3)(b_{\alpha\gamma}b_\beta b_\delta + b_{\beta\gamma}b_\alpha b_\delta)\right],\end{aligned} \tag{2.2}$$

where $b_{\alpha\beta} = \epsilon_{\alpha\beta\gamma}b_\gamma$, η_i, ζ_i are viscosity coefficients, $V_{\gamma\delta} = (\partial u_\gamma/\partial x_\delta + \partial u_\delta/\partial x_\gamma)/2$, and $\epsilon_{\alpha\beta\gamma}$ is the alternating tensor.

The physical system considered in this paper consists of an odd viscous liquid endowed with odd coefficients η_3 and η_4 in (2.2), and the field $\boldsymbol{b}$ lying in the z-direction, so $\boldsymbol{b} = \hat{\boldsymbol{z}}$.

The presentation becomes opaque when both coefficients are employed simultaneously. We thus consider each one in turn. Considering only $\eta_3 \neq 0$, we set $\eta = \eta_4 = 0$ and $\eta_2 = \eta_1 = -\zeta_1 = 0$. The corresponding odd stress tensor in polar cylindrical coordinates reads (cf. figure 2)

$$\boldsymbol{\sigma}' = \eta_o \begin{pmatrix} -\left(\partial_r v_\phi - \dfrac{1}{r}v_\phi + \dfrac{1}{r}\partial_\phi v_r\right) & \partial_r v_r - \dfrac{1}{r}v_r - \dfrac{1}{r}\partial_\phi v_\phi & 0 \\ \partial_r v_r - \dfrac{1}{r}v_r - \dfrac{1}{r}\partial_\phi v_\phi & \partial_r v_\phi - \dfrac{1}{r}v_\phi + \dfrac{1}{r}\partial_\phi v_r & 0 \\ 0 & 0 & 0 \end{pmatrix}, \tag{2.3}$$

by identifying η_o (> 0) with $-\eta_3$. In Khain *et al.* (2022), η_o also appears as coefficient $-\eta_1^o$. Since the liquid is three-dimensional, there is a third velocity component v_z, related to v_r and v_ϕ through the isochoric constraint

$$\partial_r(rv_r) + \partial_\phi v_\phi + r\,\partial_z v_z = 0. \tag{2.4}$$

For the sake of clarity, in (2.3) we have chosen only one of the coefficients that appear in the stress (2.2) to characterize our odd viscous liquid. This is done so that the fluid flow behaviour associated with this coefficient becomes uncoupled to other types. It would be possible to also consider non-zero η_4 (corresponding to η_2^o in Khain *et al.* 2022). We thus revisit the current problem in § 8 by considering the η_4 viscosity coefficient in (2.2) both individually and in conjunction with η_o.

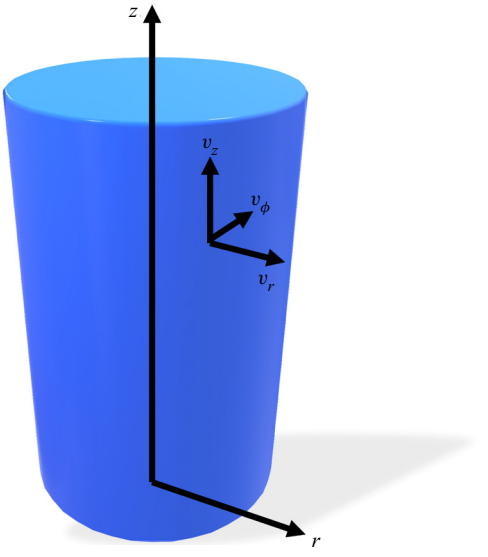

Figure 2. Three-dimensional odd viscous liquid in cylindrical coordinates, with velocity field $\boldsymbol{v} = v_r\hat{\boldsymbol{r}} + v_\phi\hat{\boldsymbol{\phi}} + v_z\hat{\boldsymbol{z}}$.

3. Three-dimensional waves in an odd viscous liquid

3.1. *Axisymmetric inertial-like waves*

In this paper, we assume tacitly the existence of an axis of anisotropy in the z-direction, established by a secondary mechanism such as a magnetic field or rotation, to which, however, we make no reference. Consider an inviscid liquid endowed with odd viscosity as in (2.3), and an axially symmetric wave propagating along the axis of the magnetic field. Following Landau & Lifshitz (1987, § 14), we consider cylindrical polar coordinates r, ϕ, z (cf. figure 2); the fields are independent of ϕ, we neglect nonlinear terms (assuming small-amplitude motions), and the time and axial dependence are given by the factor $\exp[\mathrm{i}(kz - \omega t)]$ where the frequency ω and wavenumber k along the axis are both real. Employing the constitutive law (2.3), the linearized equations of motion (see Appendix A) become

$$-\mathrm{i}\omega v_r = -\frac{1}{\rho}\frac{\partial p'}{\partial r} - \nu_o\left[\frac{1}{r}\frac{\partial}{\partial r}\left(r\frac{\partial v_\phi}{\partial r}\right) - \frac{v_\phi}{r^2}\right], \tag{3.1}$$

$$-\mathrm{i}\omega v_\phi = \nu_o\left[\frac{1}{r}\frac{\partial}{\partial r}\left(r\frac{\partial v_r}{\partial r}\right) - \frac{v_r}{r^2}\right], \tag{3.2}$$

$$-\mathrm{i}\omega v_z = -\frac{\mathrm{i}k}{\rho}p', \tag{3.3}$$

where p' is the variable part of the pressure in the wave, and ρ is the liquid's constant density. The equation of continuity is

$$\frac{1}{r}\frac{\partial}{\partial r}(rv_r) + \mathrm{i}kv_z = 0. \tag{3.4}$$

Because of (3.3) and continuity,

$$p'/\rho = \omega v_z/k = \frac{\mathrm{i}\omega}{k^2}\frac{1}{r}\frac{\partial}{\partial r}(rv_r), \tag{3.5}$$

and the identity

$$\frac{\partial}{\partial r}\left(\frac{1}{r}\frac{\partial}{\partial r}(rv_r)\right) = \frac{1}{r}\frac{\partial}{\partial r}\left(r\frac{\partial v_r}{\partial r}\right) - \frac{v_r}{r^2}, \tag{3.6}$$

we obtain

$$\frac{1}{\rho}\frac{\partial p'}{\partial r} = \frac{\mathrm{i}\omega}{k^2}\left[\frac{1}{r}\frac{\partial}{\partial r}\left(r\frac{\partial v_r}{\partial r}\right) - \frac{v_r}{r^2}\right]. \tag{3.7}$$

Thus, introducing the linear operator

$$\mathcal{L} = \partial_r^2 + \frac{1}{r}\partial_r - \frac{1}{r^2}, \tag{3.8}$$

the r and ϕ momentum equations become

$$-\mathrm{i}\omega v_r = -\mathrm{i}\frac{\omega}{k^2}\mathcal{L}v_r - \nu_o\mathcal{L}v_\phi, \tag{3.9}$$

$$-\mathrm{i}\omega v_\phi = \nu_o\mathcal{L}v_r. \tag{3.10}$$

Expressing the velocities v_r and v_ϕ in terms of Bessel or modified Bessel functions, $v_r = A\,\mathrm{J}_m(\kappa r)$, $v_\phi = B\,\mathrm{J}_m(\kappa r)$, or $v_r = A\,\mathrm{I}_m(\kappa r)$, $v_\phi = B\,\mathrm{I}_m(\kappa r)$, etc. (where A and B are constants, and κ is an eigenvalue), we find that $m = 1$. With the identity $\mathcal{L}\,\mathrm{J}_1(\kappa r) = -\kappa^2\,\mathrm{J}_1(\kappa r)$, the system (3.9) and (3.10) has a solution when the determinant $\kappa^4k^2\nu_o^2 - \omega^2(\kappa^2 + k^2)$ of the coefficients of the resulting linear system

$$Ak^2\omega - \kappa^2(\mathrm{i}\nu_o Bk^2 - A\omega) = 0 \quad \text{and} \quad \mathrm{i}\nu_o A\kappa^2 + \omega B = 0 \tag{3.11a,b}$$

vanishes. Consider first the case where the origin is included in the domain. It is not difficult to show that the solution is the Bessel function $\mathrm{J}_1(\kappa r)$ for which κ satisfies

$$\kappa^2 = \omega\,\frac{\omega \pm \sqrt{\omega^2 + (2k^2\nu_o)^2}}{2k^2\nu_o^2}. \tag{3.12}$$

Thus overall we found

$$v_r = A\,\mathrm{J}_1(\kappa r)\,\mathrm{e}^{\mathrm{i}(kz-\omega t)}, \quad v_\phi = -\mathrm{i}A\,\frac{\nu_o\kappa^2}{\omega}\,\mathrm{J}_1(\kappa r)\,\mathrm{e}^{\mathrm{i}(kz-\omega t)}, \quad v_z = \mathrm{i}A\,\frac{\kappa}{k}\,\mathrm{J}_0(\kappa r)\,\mathrm{e}^{\mathrm{i}(kz-\omega t)}. \tag{3.13a–c}$$

The motion comprises regions between coaxial cylinders with radius r_n such that

$$r_n\kappa = \gamma_n, \tag{3.14}$$

and γ_n are the zeros of $\mathrm{J}_1(x)$. Both v_r and v_ϕ vanish at these coaxial cylinders, and the fluid does not cross them. The allowed values of the frequency ω in (3.12) are not restricted in any way in the infinite medium under consideration. (In contrast, in the rotating fluid case where $\kappa = k\sqrt{4\Omega^2/\omega^2 - 1}$, the angular velocity Ω of the liquid is required to satisfy the bound $\omega < 2\Omega$, for the solution to be finite.) In defining (3.12), we have assumed tacitly that the solutions that we pursue are finite in the radial direction r and have thus

discarded κ terms associated with (exponentially increasing/decreasing) modified Bessel function solutions. The κ terms in our discussion are always real (which can be justified by choosing large ω, for instance).

Employing the radial and azimuthal momentum equations (3.1) and (3.2), we can now give a more satisfying explanation of the 'elasticity' of an odd viscous liquid and its tendency to restore a fluid particle back to its original position. Following Davidson (2013, § 1.1) and Yih (1988, § 5), consider a circular ring of fluid in an odd viscous liquid with zero shear viscosity, located wholly on the x–y plane. By some perturbation, the ring starts moving outwards with velocity $v_r > 0$, and thus expands, so that $\partial_r v_r + (1/r)v_r + (1/r)\,\partial_\phi v_\phi > 0$, where the last expression is the divergence of the velocity field in two dimensions. Rewrite (3.9)–(3.10) as

$$-\mathrm{i}\omega\left(1+\frac{\kappa^2}{k^2}\right)v_r = F_r, \quad -\mathrm{i}\omega v_\phi = F_\phi, \tag{3.15a,b}$$

where $F_r \equiv -\nu_o \mathcal{L} v_\phi = \nu_o \kappa^2 v_\phi$ and $F_\phi \equiv \nu_o \mathcal{L} v_r = -\nu_o \kappa^2 v_r$. Since $v_r > 0$, the second equation of (3.15) implies that there will be an azimuthal force $F_\phi = -\kappa^2 \nu_o v_r < 0$, an acceleration of the liquid in the $-\hat{\boldsymbol{\phi}}$ direction, and a commensurate negative velocity v_ϕ, where we employed the eigenvalue $-\kappa^2$ of the linear operator $\mathcal{L}$ in (3.8). This velocity will give rise to a radial force $F_r = -\kappa^2 \nu_o\,|v_\phi|$ in the first equation of (3.15). This force endows the ring with an acceleration that points towards the origin, that is, towards the original location of the fluid ring, so it tries to reverse its expansion (the pressure contributes the $-\mathrm{i}\omega(\kappa^2/k^2)$ term in (3.15)). As the ring passes through its original position due to inertia and contracts, $\partial_r v_r + (1/r)v_r + (1/r)\,\partial_\phi v_\phi < 0$, there will be a new azimuthal velocity component with sign opposite to the above one, that will lead to an eventual expansion towards equilibrium.

3.2. *Axial inertial-like waves interior to a cylinder*

We consider the liquid confined within a solid cylindrical surface located, say, at $r = a$, that would be realistic in a laboratory setting. This boundary will be a streamline located at an integral number of cells in the radial direction. If by γ_n we denote the nth zero of the Bessel function J_1, then (3.12) with the condition $\kappa a = \gamma_n$ leads to the constraint

$$a\left(\omega\,\frac{\omega+\sqrt{\omega^2+(2k^2\nu_o)^2}}{2k^2\nu_o^2}\right)^{1/2} = \gamma_n, \tag{3.16}$$

and n denotes the number of cells in the radial direction (cf. figure 3). From (3.16), we derive the dispersion relation

$$\omega = \frac{\nu_o k \gamma_n^2}{a\sqrt{k^2a^2+\gamma_n^2}}, \tag{3.17}$$

where n denotes the number of cells in the radial direction. (For clarity, we have suppressed the symbol $\pm$ in (3.17), and consider only the positive sign.) It is clear that in the limit $ka \gg \gamma_n$, the frequency in (3.17) becomes $\omega \sim \nu_o/a^2$, which recovers the qualitative frequency (1.4) that we obtained in the Introduction.

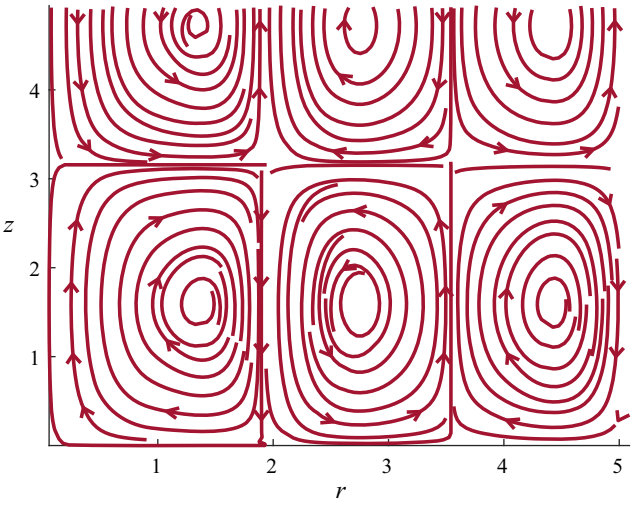

Figure 3. Instantaneous streamlines in the r–z plane with streamfunction (3.18a–c), representing a simple harmonic wave propagating in the z-direction with phase velocity $c_p = \omega/k$ (see (3.19a,b)). Vertical lines are cross-sections of cylinders wrapping around the central axis, and were formed from the zeros of the Bessel function J_1, where $v_r = 0$. The radius b of the external cylinder is determined by the condition $\kappa b = \gamma_3$, where γ_3 is the third root of the Bessel function J_1 in the streamfunction (3.18a–c), or equivalently, in the radial velocity field in (3.13a–c).

In figure 3, we plot the streamlines interior to a cylinder of radius b with the instantaneous streamfunction

$$\psi(r,z) = \frac{\kappa}{3.83}\, r\,\mathrm{J}_1(\kappa r)\sin(kz), \quad v_z = \frac{1}{r}\frac{\partial \psi}{\partial r}, \quad v_r = -\frac{1}{r}\frac{\partial \psi}{\partial z}, \tag{3.18a–c}$$

for $k = 1$ and $\kappa = 2$ for comparison with figure 7.6.4 of Batchelor (1967, p. 561), which employs the same form for the streamfunction with the first zero 3.83 of the Bessel function to modulate the amplitude in the denominator of (3.18a–c). The horizontal lines are locations where $v_r = 0$ (zeros of the Bessel function).

There is important information to be surmised from the phase and group velocities

$$c_p = \frac{v_o \gamma_n^2}{a\sqrt{k^2a^2+\gamma_n^2}} \quad \text{and} \quad c_g = \frac{v_o \gamma_n^4}{a\left(k^2a^2+\gamma_n^2\right)^{3/2}}, \tag{3.19a,b}$$

that we derive from (3.17) (we have suppressed the symbol $\pm$ and employed only the positive sign in (3.17)). Since

$$c_p = c_g + \frac{a v_o k^2 \gamma_n^2}{\left(k^2a^2+\gamma_n^2\right)^{3/2}} > c_g, \tag{3.20}$$

the energy of a disturbance caused by a slowly moving body along the axis of the cylinder, with velocity c_p, cannot advance upstream relative to the body. Waves will be formed in the downstream direction. We reach the analogous conclusion if we employ the negative sign in (3.17). This situation is thus similar to the rotating liquid case, where the energy cannot propagate upstream and thus waves are formed only downstream, as described in many experiments, e.g. those of Long (1953). We verify these claims in § 3.4 by combining numerical simulations of the Navier–Stokes equations with the theoretical predictions of

the present subsection. (Note how the expression for ω in (3.17) contrasts with the inviscid liquid rotating at angular velocity Ω, where $\omega = 2\Omega k/\sqrt{k^2 + (\gamma_n/a)^2}$.)

3.3. *Allowed wavenumbers*

When the number of cells in the radial direction is n, from (3.16) allowed wavenumbers supporting propagation with phase velocity $c_p = \omega/k$, and for which the boundary at $r = a$ is a streamline, satisfy

$$ak = \gamma_n \left(\left(\frac{\nu_o \gamma_n}{a c_p} \right)^2 - 1 \right)^{1/2}. \tag{3.21}$$

Wave propagation is thus possible when

$$\frac{a c_p}{\nu_o} < \gamma_n, \tag{3.22}$$

where n denotes the number of cells in the radial direction. Thus although (3.12) does not introduce a restriction on frequencies for the propagation of waves, (3.21) does: defining a Maxworthy number $\mathcal{M}_a$ based on the phase velocity c_p and cylinder radius a (cf. (6.2*a*,*b*) for the definition of the dimensionless number $\mathcal{M}$),

$$\mathcal{M}_a = \frac{\nu_o}{a c_p}, \tag{3.23}$$

inertial motions with n cylinders (nth zero of J_1) are possible only when

$$\mathcal{M}_a > \frac{1}{\gamma_n}. \tag{3.24}$$

3.4. *Numerical determination of odd viscous inertial oscillations inside a cylinder of radius a*

By the inequality (3.20), we argued that, based on the inertial-like waves construction of §§ 3.1–3.3, the energy of a disturbance caused by a slowly moving body along the axis of the cylinder, with velocity c_p, cannot advance upstream relative to the body. Waves will be formed in the downstream direction.

To verify this claim, we perform numerical simulations of the full Navier–Stokes equations of a slowly moving body with velocity $U = 0.05\,\mathrm{cm\,s^{-1}}$ in a cylinder of base radius $a = 25\,\mathrm{cm}$ filled with an odd viscous liquid of dynamic coefficient $\eta_o = 0.7\,\mathrm{g\,(cm\,s)^{-1}}$, shear viscosity $\eta = 0.01\,\mathrm{g\,(cm\,s)^{-1}}$ and density $\rho = 1.1\,\mathrm{g\,cm^{-3}}$. Figure 4(*b*) displays the streamlines in the r–z plane of the liquid downstream of the moving body, which show wave-like behaviour. To determine the wavelength, the colour bar shows the strength of the radial liquid velocity v_r whose direction changes sign as we move down. From the plot, we can determine visually that the wavelength λ is approximately 25 cm. We compare this estimate to the theoretical prediction of §§ 3.1–3.3:

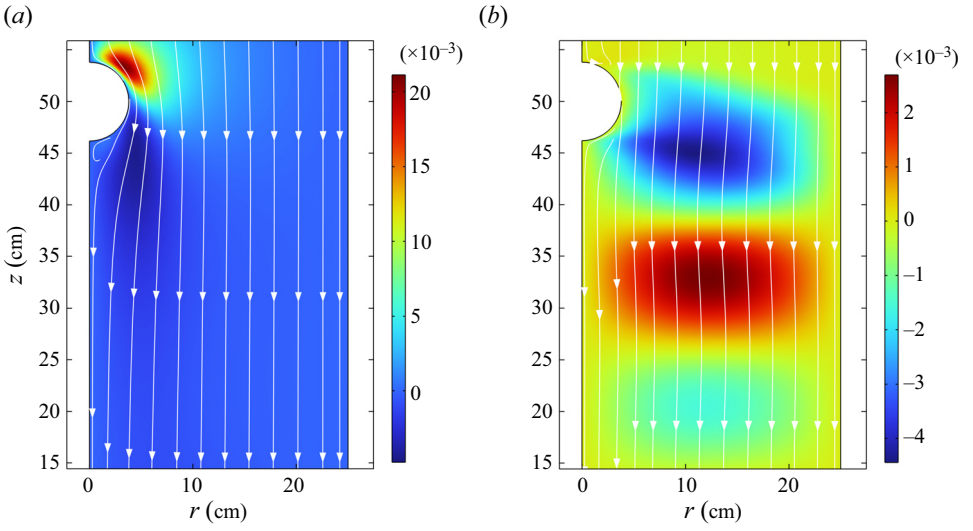

Figure 4. (*a*) In the absence of odd viscosity, no radial disturbance is visible as we move down and away from the body. The colour bar denotes radial velocity. The plot was produced with the finite-element package comsol by solving the full Navier–Stokes equations including inertial terms in a three-dimensional axisymmetric domain. (*b*) Waves generated by a small (3.8 cm) slowly-moving sphere (located at the centre of the cylinder – upper left of the plot) in an odd viscous liquid contained in a cylinder of radius 25 cm. The colour bar denotes the strength of the radial liquid velocity v_r. Its direction changes sign as we move down and away from the body, and it is thus responsible for the distortion of the streamlines (in white). From this plot, we can determine visually the wavelength to be approximately 25 cm. This agrees rather well with the theoretical estimate 24.476 cm obtained from (3.25).

from (3.21), we find that

$$\lambda = \frac{2\pi}{k} = \frac{2\pi a}{\gamma_1 \sqrt{\left(\dfrac{\nu_o \gamma_1}{aU}\right)^2 - 1}} = 24.4764\,\text{cm}, \tag{3.25}$$

where $\gamma_1 = 3.8317$ is the first root of the Bessel function J_1. Figure 4(*a*) displays the same system as in figure 4(*b*) but with $\eta_o = 0$. No radial disturbance is visible in this case. Figure 4 was produced with the finite-element package comsol by solving the full Navier–Stokes equations in a three-dimensional axisymmetric domain. The flow Reynolds number, based on cylinder radius $a = 25$ cm, is 125.

This situation is thus analogous to the rotating liquid case where the energy cannot propagate upstream and thus waves are formed only downstream, as described by the experiments of Long (1953); cf. Batchelor (1967, pp. 564–566 and plate 24).

3.5. *Axial inertial-like waves exterior to a cylinder*

The above discussion can also be employed to establish wave propagation when the odd viscous liquid occupies the region $r > a$, exterior to a solid cylinder located at $r = a$. Now, the solution is of the form of a Bessel function of the second kind in the radial coordinate,

$$v_r = A\,\mathrm{Y}_1(\kappa r)\,\mathrm{e}^{\mathrm{i}(kz-\omega t)}, \quad v_\phi = -\mathrm{i}A\,\frac{\nu_o \kappa^2}{\omega}\,\mathrm{Y}_1(\kappa r)\,\mathrm{e}^{\mathrm{i}(kz-\omega t)}, \quad v_z = \mathrm{i}A\,\frac{\kappa}{k}\,\mathrm{Y}_0(\kappa r)\,\mathrm{e}^{\mathrm{i}(kz-\omega t)}, \tag{3.26a–c}$$

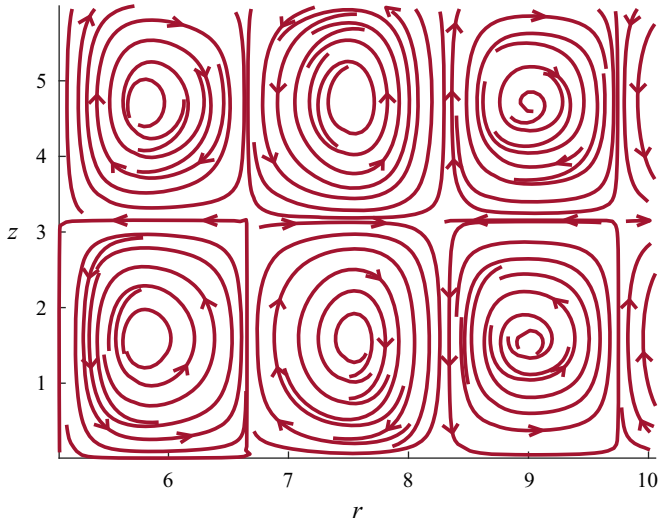

Figure 5. Instantaneous streamlines exterior to a cylinder of radius $r = \alpha_3/\kappa$, where α_3 is the third zero of Y_1. This is a simple harmonic wave propagating in the z-direction with phase velocity ω/k. Vertical lines correspond to zeros of the Bessel function of the second kind Y_1, where $v_r = 0$.

and the results of the previous subsections hold with the replacement

$$\mathrm{J}_1 \to \mathrm{Y}_1, \quad \gamma_n \to \alpha_n, \tag{3.27a,b}$$

where α_n is the nth zero of $\mathrm{Y}_1(x)$. In figure 5, we plot the streamlines exterior to a cylinder of radius b with the instantaneous streamfunction

$$\psi(r,z) = \frac{\kappa}{3.83}\, r\, \mathrm{Y}_1(\kappa r)\sin(kz), \quad v_z = \frac{1}{r}\frac{\partial \psi}{\partial r}, \quad v_r = -\frac{1}{r}\frac{\partial \psi}{\partial z}, \tag{3.28a–c}$$

for $k = 1$ and $\kappa = 2$ for comparison with figure 7.6.4 of Batchelor (1967, p. 561).

3.6. *Plane-polarized waves induced by odd viscosity*

The axisymmetric inertial-like waves that we discussed earlier propagate along the z axis (the axis of anisotropy) and are three-dimensional in the sense that the wave amplitude varies along both the propagation direction and normal to it. In this subsection, we will consider different types of inertial-like waves that propagate along an arbitrary direction $\hat{\boldsymbol{k}}$ and are polarized in the plane perpendicular to the propagation axis. This subsection follows the notation of Landau & Lifshitz (1987, § 14). The odd-viscous Navier–Stokes equations

$$\frac{\mathrm{D}\boldsymbol{v}}{\mathrm{D}t} = -\frac{1}{\rho}\boldsymbol{\nabla} p + \nu_o\, \nabla_2^2 \hat{\boldsymbol{z}} \times \boldsymbol{v}, \tag{3.29}$$

where $\nabla_2^2 = \partial_x^2 + \partial_y^2$ and $\mathrm{D}/\mathrm{D}t$ is the convective derivative, become, after taking the curl of both sides,

$$\frac{\mathrm{D}}{\mathrm{D}t}\mathrm{curl}\,\boldsymbol{v} = (\mathrm{curl}\,\boldsymbol{v})\cdot\boldsymbol{\nabla}\boldsymbol{v} - \nu_o\,\nabla_2^2\frac{\partial \boldsymbol{v}}{\partial z}. \tag{3.30}$$

Linearizing,

$$\partial_t\,\mathrm{curl}\,\boldsymbol{v} = -\nu_o\,\nabla_2^2\frac{\partial \boldsymbol{v}}{\partial z}, \tag{3.31}$$

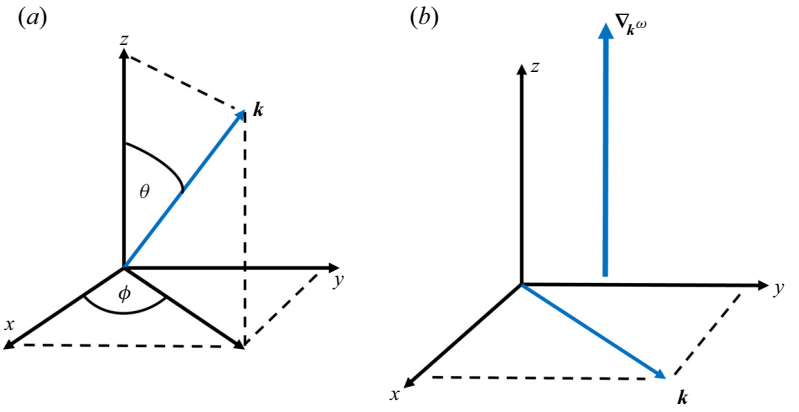

Figure 6. (*a*) Coordinate system employed in plane-polarized waves, showing the definition of angles for the propagation wavevector $\boldsymbol{k}$. (*b*) When the propagation direction is normal to the axis $\hat{\boldsymbol{z}}$, the group velocity $\boldsymbol{c}_g = \nabla_{\boldsymbol{k}}\omega$ in (3.41) becomes co-axial to the axis $\hat{\boldsymbol{z}}$, and acquires its maximum value.

we seek plane-wave solutions of the form

$$\boldsymbol{v} = \boldsymbol{A}\exp(\mathrm{i}(\boldsymbol{k}\cdot\boldsymbol{r} - \omega t)), \tag{3.32}$$

where $\boldsymbol{A}$ is normal to $\boldsymbol{k}$ from the incompressibility condition.

Substituting the plane-wave solution into (3.31), we obtain

$$\omega\boldsymbol{k}\times\boldsymbol{v} = \mathrm{i}\nu_o(k_x^2 + k_y^2)k_z\boldsymbol{v}. \tag{3.33}$$

Taking the cross-product of both sides of (3.33) with $\boldsymbol{k}$, we obtain

$$-\omega k^2\boldsymbol{v} = \mathrm{i}\nu_o(k_x^2 + k_y^2)k_z\boldsymbol{k}\times\boldsymbol{v}. \tag{3.34}$$

System (3.33)–(3.34) has a solution when the determinant of the coefficients vanishes. Solving for ω, we obtain

$$\omega = \pm\frac{\nu_o(k_x^2 + k_y^2)k_z}{k}, \quad \text{or} \quad \omega = \pm\nu_o k^2\cos\theta\sin^2\theta, \tag{3.35}$$

where $k = \sqrt{k_x^2 + k_y^2 + k_z^2}$, and the latter equation implies that θ is the angle between $\boldsymbol{k}$ and the anisotropy axis (cf. figure 6). In figure 7, we plot the dispersion ω (see (3.35)) versus angle θ between the wavevector $\boldsymbol{k}$ and the z (anisotropy) axis. It differs qualitatively from the corresponding relation

$$\omega = 2\Omega\cos\theta \tag{3.36}$$

of a (non-odd viscous) inviscid fluid rotating with angular velocity Ω; cf. Greenspan (1968). Comparing (3.35) with (3.36), when the coefficients ν_o and Ω are kept constant, it becomes evident that the dispersion relation (3.35) obtained due to the specific form of the constitutive law (2.3) that we adopted for an odd viscous liquid becomes prominent for large in-plane wavenumbers and small corresponding wavelengths.

Following Landau & Lifshitz (1987), we introduce the unit vector $\hat{\boldsymbol{k}} = \boldsymbol{k}/k$ in the direction of the wavevector, and the complex amplitude $\boldsymbol{A} = \boldsymbol{a} + \mathrm{i}\boldsymbol{b}$, where $\boldsymbol{a}$ and $\boldsymbol{b}$ are real vectors. Considering (3.33) and the dispersion relation (3.35), we obtain $\hat{\boldsymbol{k}}\times\boldsymbol{b} = \boldsymbol{a}$,

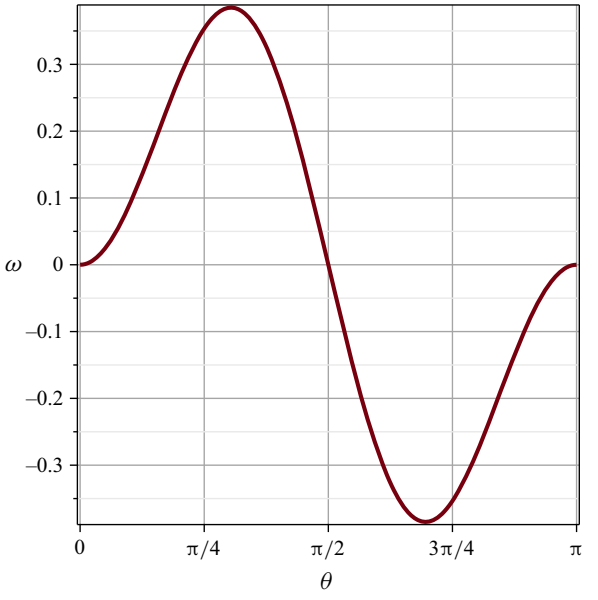

Figure 7. Subsection 3.6 plane-polarized wave dispersion ω (see (3.35)) versus angle θ between the wavevector $\boldsymbol{k}$ and the z (anisotropy) axis (setting $k = \nu_o = 1$). Of interest is the low-frequency range at $\theta \sim \pi/2$ where group velocity is maximum. This curve structure should be contrasted to the corresponding relation $\omega = 2\Omega\cos\theta$ of an inviscid fluid rotating with angular velocity Ω.

that is, the two vectors $\boldsymbol{a}$ and $\boldsymbol{b}$ are perpendicular to each other, are of the same magnitude, and lie in the plane whose normal is $\boldsymbol{k}$. Thus the velocity field is polarized circularly in the plane defined by $\boldsymbol{a}$ and $\boldsymbol{b}$, and is of the form

$$\boldsymbol{v} = \boldsymbol{a}\cos(\boldsymbol{k}\cdot\boldsymbol{r} - \omega t) - \boldsymbol{b}\sin(\boldsymbol{k}\cdot\boldsymbol{r} - \omega t), \quad \boldsymbol{a} \perp \boldsymbol{b}. \tag{3.37}$$

Employing the negative sign of the dispersion relation (3.35), the above analysis leads to the same velocity field (3.37) but with the sense of the vectors $\boldsymbol{a}$ and $\boldsymbol{b}$ reversed: $\hat{\boldsymbol{k}} \times \boldsymbol{b} = -\boldsymbol{a}$. This will become important in § 4, where the helicity associated with wave propagation will be determined.

It is of interest to calculate the direction of propagation of energy. We obtain

$$\frac{\partial\omega}{\partial k_x} = \nu_o\frac{k_x k_z(k^2 + k_z^2)}{k^3}, \quad \frac{\partial\omega}{\partial k_y} = \nu_o\frac{k_y k_z(k^2 + k_z^2)}{k^3}, \quad \frac{\partial\omega}{\partial k_z} = \nu_o\frac{(k_x^2 + k_y^2)^2}{k^3}, \tag{3.38a–c}$$

or, taking the z axis to be the axis of anisotropy,

$$\left(\frac{\partial\omega}{\partial k_x}, \frac{\partial\omega}{\partial k_y}\right) = k\nu_o\sin\theta\cos\theta(1 + \cos^2\theta)(\cos\phi, \sin\phi), \quad \frac{\partial\omega}{\partial k_z} = k\nu_o\sin^4\theta. \tag{3.39a,b}$$

The group velocity $\boldsymbol{c}_g = \partial\omega/\partial\boldsymbol{k}$ in vector form can be written as

$$\frac{\partial\omega}{\partial\boldsymbol{k}} = \nu_o k\left\{\hat{\boldsymbol{k}}(\hat{\boldsymbol{z}}\cdot\hat{\boldsymbol{k}})\left[1 + (\hat{\boldsymbol{z}}\cdot\hat{\boldsymbol{k}})^2\right] + \hat{\boldsymbol{z}}\left[1 - 3(\hat{\boldsymbol{z}}\cdot\hat{\boldsymbol{k}})^2\right]\right\}, \tag{3.40}$$

which can be compared with its rigidly rotating (non-odd viscous) counterpart $\partial\omega/\partial\boldsymbol{k} = (2\Omega/k)[\hat{\boldsymbol{z}} - \hat{\boldsymbol{k}}(\hat{\boldsymbol{z}}\cdot\hat{\boldsymbol{k}})]$, where the group velocity is perpendicular to the phase

	Odd viscous liquid	Rigidly rotating liquid
Low ω	$\boldsymbol{k} \parallel \boldsymbol{\Omega}$, $c_g = 0$, and $\boldsymbol{k} \perp \boldsymbol{\Omega}$, $\boldsymbol{c}_g = \pm\nu_o k\hat{\boldsymbol{z}}$ (max)	$\boldsymbol{k} \perp \boldsymbol{\Omega}$, $\boldsymbol{c}_g = \dfrac{\pm 2\Omega\hat{\boldsymbol{z}}}{k}$ (max)
High ω	$\theta = \cos^{-1}(\sqrt{3}/3) \sim 0.3\pi$	$\boldsymbol{k} \parallel \boldsymbol{\Omega}$, $\boldsymbol{c}_g = 0$
$\boldsymbol{c}_p \cdot \boldsymbol{c}_g$	$2\,\lvert\boldsymbol{c}_p\rvert^2$	0
$\boldsymbol{v} \cdot \operatorname{curl} \boldsymbol{v}$	$\mp k\,\lvert\boldsymbol{v}\rvert^2$	$\mp k\,\lvert\boldsymbol{v}\rvert^2$

Table 1. Summary of odd viscous plane-polarized inertial-like wave behaviour at low and high frequencies (see (3.35)) and comparison with their rigidly rotating counterparts. Here, $\boldsymbol{c}_g$ is the group velocity $\partial\omega/\partial\boldsymbol{k}$, and $\boldsymbol{c}_p = (\omega/k)\hat{\boldsymbol{k}}$ is the phase velocity. The group velocity is maximum when the angle is $\theta = \pi/2$, propagation takes place perpendicular to the anisotropy axis ($\hat{\boldsymbol{z}}$), the group velocity acquires its maximum propagation along the anisotropy axis, and helicity becomes segregated; cf. § 4. Helicity density $\boldsymbol{v} \cdot \operatorname{curl} \boldsymbol{v}$ has the same functional form in both odd viscous and rigidly rotating liquids. Although in a rigidly rotating liquid the group velocity is always perpendicular to the phase velocity, in an odd viscous liquid there is dependence on the angle θ (see the third row of the table), were θ denotes the angle between $\boldsymbol{\Omega} = \Omega\hat{\boldsymbol{z}}$ and the propagation direction $\boldsymbol{k}$; cf. figure 6.

velocity $\boldsymbol{c}_p = (\omega/k)\hat{\boldsymbol{k}}$ (see table 1). Here, the group velocity is not perpendicular to the phase velocity. A calculation gives $\boldsymbol{c}_g \cdot \boldsymbol{c}_p = 2|\boldsymbol{c}_p|^2 = 2\nu_o^2 k^2 \cos^2\theta \sin^4\theta$. Thus, in contrast to the case of inertial waves in a rotating fluid where the energy propagates perpendicularly to the wavevector, here the energy propagation direction has a component along the $\hat{\boldsymbol{k}}$ axis. The modulus of the group velocity is

$$\left|\frac{\partial\omega}{\partial\boldsymbol{k}}\right| = k\nu_o \sin\theta\sqrt{5\cos^4\theta - 2\cos^2\theta + 1}. \tag{3.41}$$

In figure 8, we plot the group velocity components (3.39*a*,*b*) and its magnitude (3.41) versus angle θ between the wavevector $\boldsymbol{k}$ and the z (anisotropy) axis (setting $k = \nu_o = 1$).

In addition to the information in table 1, the frequency is maximum at $\theta = \cos^{-1}(\sqrt{3}/3) \sim 0.3\pi$, acquiring the value $\omega = \pm\nu_o k^2(2\sqrt{3}/9)$. The group velocity becomes $(4k\nu_o/9)(\sqrt{2}\cos\phi, \sqrt{2}\sin\phi, 1)$, and its modulus is $c_g = 4k\nu_o\sqrt{3}/9$. In addition, the group velocity has a local maximum at $\theta = \cos^{-1}(\sqrt{15}/5) \sim 0.22\pi$. The frequency is $\omega = \pm\nu_o k^2(2\sqrt{15}/25)$, and the group velocity becomes $(4k\nu_o/25)(2\sqrt{6}\cos\phi, 2\sqrt{6}\sin\phi, 1)$, with modulus $c_g = 4k\nu_o/5$. Comparison can be made of (3.41) with plane-polarized waves rotating rigidly (Landau & Lifshitz 1987, § 14), where $|\partial\omega/\partial\boldsymbol{k}| = (2\Omega/k)\sin\theta$.

4. Conservation of helicity of inertial-like waves in an odd viscous liquid

Helicity

$$\mathcal{H} = \int_V \boldsymbol{v} \cdot \operatorname{curl} \boldsymbol{v}\, \mathrm{d}V = \text{constant} \tag{4.1}$$

was shown by Moffatt (1969) to be an invariant of inviscid fluid motion when $\hat{\boldsymbol{n}} \cdot \operatorname{curl} \boldsymbol{v}$ vanishes on any closed orientable surface moving with the liquid. Here, we show that, analogously to the rigidly rotating case, the vorticity of an odd viscous liquid is proportional to the velocity field. For plane-polarized inertial-like waves, this implies that helicity is conserved. Since a number of effects appearing in the literature, such as the emission of inertial waves in a turbulent flow (Davidson 2013, figure 3.3(*b*)), are related

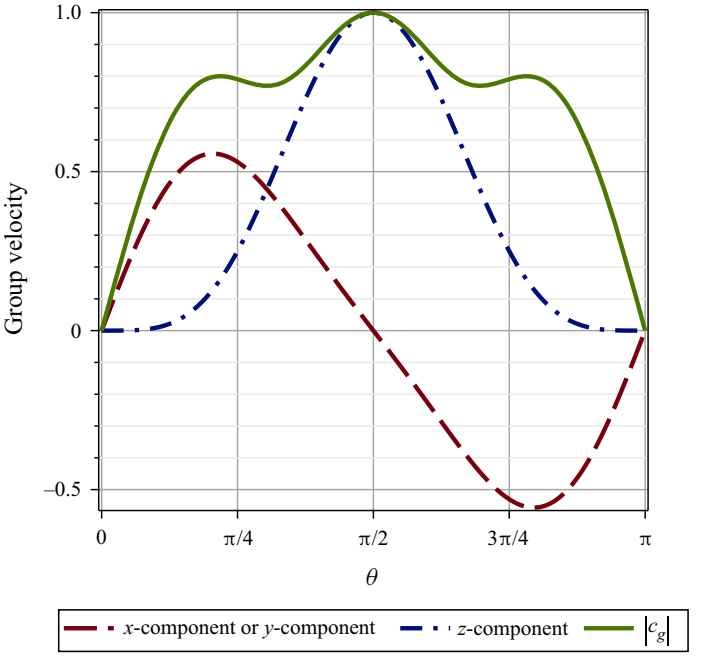

Figure 8. Subsection 3.6 plane-polarized wave group velocity components and magnitude (3.39*a*,*b*) and (3.41) versus angle θ between the wavevector $\boldsymbol{k}$ and the z (anisotropy) axis, setting $k = \nu_o = 1$ (and $\phi = \pi/4$, for simplicity). Of interest is the low-frequency range at $\theta \sim \pi/2$, where group velocity is maximum. The modulus of the group velocity should be contrasted to $|\partial\omega/\partial\boldsymbol{k}| = (2\Omega/k)\sin\theta$ in the case of an inviscid rigidly rotating liquid with angular velocity Ω.

to helicity and its sign, we include some discussion below on the presence of helicity in odd-viscosity-induced inertial-like waves.

4.1. *Conservation of helicity in plane-polarized waves of an odd viscous liquid*

From the plane-polarized velocity field (3.37), we obtain $\operatorname{curl}\boldsymbol{v} = -\boldsymbol{k}\times\boldsymbol{b}\cos(\boldsymbol{k}\cdot\boldsymbol{r}-\omega t) - \boldsymbol{k}\times\boldsymbol{a}\sin(\boldsymbol{k}\cdot\boldsymbol{r}-\omega t)$. The relation $\hat{\boldsymbol{k}}\times\boldsymbol{b} = \pm\boldsymbol{a}$ (where the $\pm$ symbol corresponds to the sign of the dispersion relation (3.35)) leads to $\operatorname{curl}\boldsymbol{v} = \mp k\boldsymbol{v}$, thus

$$\boldsymbol{v}\cdot\operatorname{curl}\boldsymbol{v} = \mp k\,|\boldsymbol{v}|^2 \quad\text{and}\quad \mathcal{H} = \int_V \boldsymbol{v}\cdot\operatorname{curl}\boldsymbol{v}\,\mathrm{d}V = \mp k\,|\boldsymbol{v}|^2\,V, \tag{4.2a,b}$$

where $|\boldsymbol{v}|^2 = |\boldsymbol{a}|^2 + |\boldsymbol{b}|^2$ is the constant magnitude of the velocity in (3.37), V is the volume of the region under consideration, and $k = \sqrt{k_x^2 + k_y^2 + k_z^2}$. The negative sign in (4.2*a*,*b*) (corresponding to the positive sign in the dispersion relation (3.35)) is associated with particle paths following left-handed helices, and the positive sign is associated with right-handed helices. Energy propagates along a cone whose normal is the vector $\hat{\boldsymbol{k}}$ (cf. Davidson (2013) for the case of a rigidly rotating liquid).

Inertial-like waves give rise to maximal helicity. This can be seen by substituting (4.2*a*,*b*) into the the Cauchy–Schwarz inequality $\mathcal{H}^2 \le \mathcal{E}\mathcal{W}$ expressed in terms of the

helicity (4.1) and the energy and enstrophy integrals (Moffatt 1969)

$$\mathcal{E} = \int_V \boldsymbol{v}^2 \,\mathrm{d}V, \quad \mathcal{W} = \int_V (\operatorname{curl} \boldsymbol{v})^2 \,\mathrm{d}V. \tag{4.3a,b}$$

As shown by Moffatt (1970) for the case of rigidly rotating liquids, inertial waves exhibit a loss of reflection symmetry when the energy propagates parallel to the rotation axis (and the phase velocity is perpendicular to this axis). Davidson (2013) associates each direction of propagation of energy with one of the signs of helicity in (4.2*a*,*b*): negative sign of helicity for energy propagating in the $+\hat{\boldsymbol{z}}$ direction, and positive sign of helicity for energy propagating in the $-\hat{\boldsymbol{z}}$ direction. This is called the 'segregation of helicity' and has found applications in problems of magnetohydrodynamics (Davidson 2013; Davidson & Ranjan 2018). The waves that correspond to this type of behaviour have low frequencies (the frequency ω in (3.35) is nearly zero). The consequence of this behaviour in an odd viscous liquid can be seen more easily by going back to the original equation of motion (3.29). Linearizing, and taking the limit $\omega \to 0$, amounts to dropping the time derivative. Then the equation of motion becomes (5.1*a–c*) of the next section, which makes the dynamics effectively two-dimensional (perpendicular to the anisotropy axis), leads to the Taylor–Proudman theorem, and gives rise to Taylor columns.

4.2. *Helicity in axisymmetric inertial-like waves of an odd viscous liquid*

It turns out that vorticity is also parallel to the velocity field for the inertial-like waves of § 3.1. This can be shown directly by taking the curl of the velocity field (3.13*a–c*) and solving in expression (3.12) for the frequency $\omega = \nu_o k\kappa^2/\sqrt{k^2+\kappa^2}$. (In contrast to the previous section, k here denotes the wavenumber k_z along the axis; cf. § 3.1.) Alternatively, setting $A = a\,\mathrm{e}^{\mathrm{i}\theta}$ for real amplitude a and phase θ, we obtain

$$v_r = a\,\mathrm{J}_1(\kappa r)\cos(kz-\omega t+\theta), \quad v_\phi = \frac{\nu_o\kappa^2}{\omega}\,a\,\mathrm{J}_1(\kappa r)\sin(kz-\omega t+\theta), \tag{4.4a,b}$$

and $v_z = -(\kappa/k)a\,\mathrm{J}_0(\kappa r)\sin(kz-\omega t+\theta)$. In either case, the final result is

$$\operatorname{curl}\boldsymbol{v} = \mp\sqrt{k^2+\kappa^2}\,\boldsymbol{v} \quad \text{and} \quad \boldsymbol{v}\cdot\operatorname{curl}\boldsymbol{v} = \mp\sqrt{k^2+\kappa^2}\,|\boldsymbol{v}|^2. \tag{4.5a,b}$$

When the liquid is contained in a solid cylinder of radius b, ω is replaced by (3.17) and κ by γ_n/b, where γ_n is the nth zero of $\mathrm{J}_1(x)$.

5. Modified Taylor–Proudman theorem

For simplicity, we consider Cartesian coordinates. The 'geostrophic' form (i.e. Navier–Stokes with odd viscosity, without inertia and without shear viscosity) of the equations is

$$\frac{1}{\rho}\frac{\partial p}{\partial x} = -\nu_o\,\nabla_2^2 v, \quad \frac{1}{\rho}\frac{\partial p}{\partial y} = \nu_o\,\nabla_2^2 u, \quad \frac{\partial p}{\partial z} = 0, \tag{5.1a–c}$$

where $\nabla_2^2 = \partial_x^2 + \partial_y^2$. This reduction is possible by invoking the requirement $u \ll \nu_o/\ell$, where u and ℓ are characteristic velocity and length scales, respectively. This inequality

can be derived by balancing the inertial terms $\boldsymbol{v}\cdot\boldsymbol{\nabla}\boldsymbol{v}\sim u^2/\ell$ with the odd viscous term $\nu_o\nabla_2^2 u\sim\nu_o u/\ell^2$, and requiring that latter is dominant, or in other words,

$$|\boldsymbol{v}\cdot\boldsymbol{\nabla}\boldsymbol{v}|\ll|\nu_o\nabla_2^2\boldsymbol{v}|\quad\text{and}\quad|\nu_e\nabla^2\boldsymbol{v}|\ll|\nu_o\nabla_2^2\boldsymbol{v}|,\tag{5.2a,b}$$

where the latter inequality implies subdominance of shear viscosity with respect to odd viscosity. These two inequalities lead us to define new dimensionless Taylor $\mathcal{T}$ and Maxworthy $\mathcal{M}$ parameters that will be discussed in the next section (see (6.2a,b)).

Differentiating (5.1a,b) with respect to z and considering (5.1c), we obtain

$$\nabla_2^2\partial_z u=0\quad\text{and}\quad\nabla_2^2\partial_z v=0.\tag{5.3a,b}$$

Eliminating the pressure by cross-differentiation of (5.1a,b), we obtain

$$\nabla_2^2(\partial_x u+\partial_y v)=0.\tag{5.4}$$

Thus, from continuity we also obtain

$$\nabla_2^2\partial_z w=0.\tag{5.5}$$

Defining

$$(U,V,W)=\ell^2\nabla_2^2(u,v,w)\tag{5.6}$$

(the length scale is determined, for instance from the size of the vessel), we derive the Taylor–Proudman theorem for the velocity field (U,V,W), that is,

$$\partial_z U=\partial_z V=\partial_z W=0,\tag{5.7}$$

and this can be considered as a liquid in a frame rotating with angular velocity $\Omega=\nu_o\ell^{-2}$. Thus when the odd viscosity terms are larger than inertia, there is a superposition of a two-dimensional motion in the lateral x–y plane and a vertical motion, independent of z.

Some familiar behaviour at a boundary can also be recovered. Because of the no-penetration condition $w=0$ on a solid boundary, we have $W=0$ on the same boundary ($(\partial_x^2+\partial_y^2)w$ must be zero on the boundary). Thus when a streamline parallel to the axis meets a stationary boundary, this implies that W is zero everywhere.

For axisymmetric systems, a further simplification takes place. Letting $V_r=\mathcal{L}v_r$ and $V_\phi=\mathcal{L}v_\phi$, where $\mathcal{L}$ was defined in (3.8), (5.1a–c) become

$$\nu_o V_\phi=-\frac{1}{\rho}\frac{\partial p}{\partial r}\quad\text{and}\quad-\nu_o V_r=0.\tag{5.8a,b}$$

Thus V_r is zero everywhere, and the flow proceeds in spirals. With $V_z=\mathcal{L}v_z$, the continuity equation becomes $\partial_r V_r+\partial_z V_z=0$. Thus $\partial_z V_z=0$ everywhere, giving rise to the Taylor–Proudman theorem.

6. Taylor columns in an odd viscous liquid

The Navier–Stokes equations (5.1a–c) written in the form

$$\frac{1}{\rho}\frac{\partial p}{\partial x}=-\frac{\nu_o}{a^2}V,\quad\frac{1}{\rho}\frac{\partial p}{\partial y}=\frac{\nu_o}{a^2}U,\quad\frac{\partial p}{\partial z}=0,\tag{6.1a–c}$$

by employing the definitions of U, V and W in (5.6), are suggestive of the existence of Taylor columns in an odd viscous liquid. By this we mean that when an axisymmetric

body moves slowly in an odd viscous liquid, a column or a 'slug' will be pushed ahead of the body with zero axial velocity relative to the body. In the inviscid limit implied by (6.1*a–c*) (meaning that the shear viscosity is zero), the column is a cylinder, but it will be modified by the presence of shear viscosity. A rear slug will also be present. In general, the motion of the liquid in the slug cannot be determined from the simple equations (6.1*a–c*). In reality, a number of boundary layers exist that act as a conduit that transports liquid between different locations.

The determination of the flow structure is not only difficult but also changes dramatically when one alters the parameters and the geometry. Taylor columns were studied in the past in the context of slowly moving bodies immersed in a liquid rotating rigidly; see, for instance, the comprehensive articles Moore & Saffman (1968), Maxworthy (1970), Bush, Stone & Tanzosh (1995) and Tanzosh & Stone (1994), and references therein.

We can define some useful dimensionless parameters for the odd-viscosity-dominated problems, such as the Taylor $\mathcal{T}$ and Maxworthy $\mathcal{M}$ numbers (Maxworthy (1970) employed the notation N to denote the rotating counterpart of the latter):

$$\mathcal{T} = \frac{\nu_o}{\nu_e}, \quad \mathcal{M} = \frac{\nu_o}{aU}. \tag{6.2a,b}$$

To understand how (6.1*a–c*) arise, we introduce dimensionless variables

$$\boldsymbol{X} = \frac{\boldsymbol{x}}{a}, \quad T = \frac{Ut}{a}, \quad \mathcal{V} = \frac{\boldsymbol{v}}{U}, \quad P = \frac{pa}{\rho \nu_o U}, \tag{6.3a–d}$$

and the dimensionless form of the Navier–Stokes equations that includes shear viscosity, scaled by the velocity U and size a of a slowly moving body, becomes

$$\mathcal{M}^{-1} \frac{\mathrm{D}\mathcal{V}}{\mathrm{D}T} = -\boldsymbol{\nabla} P + \nabla_2^2 \hat{\boldsymbol{z}} \times \mathcal{V} + \mathcal{T}^{-1} \nabla^2 \mathcal{V}, \tag{6.4}$$

where the gradient operators refer to the dimensionless variables (6.3*a–d*). In the limit of Taylor and Maxworthy numbers $\mathcal{T}, \mathcal{M} \gg 1$, as defined in (6.2*a,b*), one obtains (6.1*a–c*).

The Taylor number can be understood as an inverse Ekman number denoting the strength of odd to even viscosity (angular velocity to even viscosity in the rotating fluid case), and the Maxworthy number is the ratio of odd viscous force to inertial forces or the odd-viscosity-induced inertial wave propagation velocity to convection velocity.

We can compare the Maxworthy number $\mathcal{M}$ in (6.2*a,b*) for an odd viscous liquid to the inverse Rossby number $Ro^{-1} = \Omega a/U$ in (B1*a,b*) when the parameters ν_o and Ω are held constant. It is clear that Taylor columns in an odd viscous liquid are favoured at small (in-plane) length scales, while Taylor columns are favoured at large length scales in rigidly rotating liquids. This is clear due to the fact that odd viscosity multiplies second-order spatial derivatives. Even if its value is small and unimportant in general, observable effects will be present close to boundaries, such as sharp boundary layers. Thus one should consider odd viscous effects (described by the specific constitutive law (2.3)) under the restrictions posed by this discussion, which might limit the applicability of the odd viscous liquids in comparison to their (non-odd viscous) rotating counterparts.

The pressure p is a streamfunction and thus constant on a streamline of the flow (U, V, W). A finite-length cylinder with generators parallel to the rotating axis and moving horizontally in a rotating liquid will have a liquid velocity parallel to its generators, and a column will accompany its motion (Yih 1988, § 12.2). Likewise, a solid body translating slowly along the axis of the cylinder will be accompanied by a column of fluid with generators parallel to the axis.

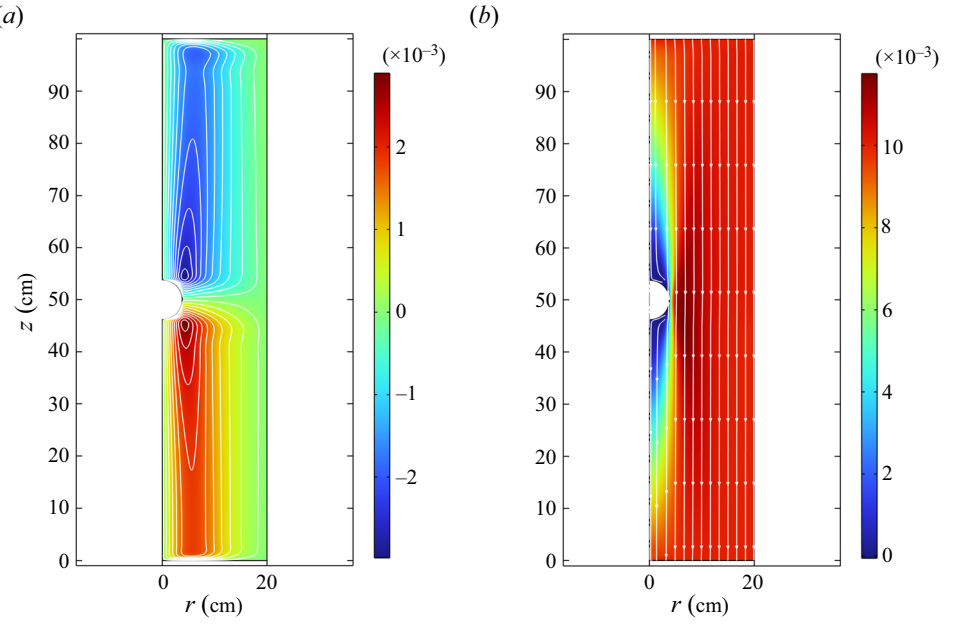

Figure 9. Distribution of (*a*) azimuthal and (*b*) axial velocity in an odd liquid moving slowly and meeting an immobile sphere (of radius 3.8 cm) located at elevation $z = 50$ cm at the centre axis of a cylinder. Liquid enters from the top ($z = 100$ cm) and exits at the bottom ($z = 0$). The sphere is not allowed to rotate. Counter-rotation of liquid takes place above and below the sphere in the azimuthal direction (this was also observed by Khain *et al.* (2022, figure 4*c*) for the analogous problem in Stokes flow). A Taylor-type column is also visible in (*b*), placed symmetrically above and below the sphere.

Figures 9 and 10 display the salient features of Taylor columns in odd viscous liquids. Liquid flow entering from the top of a cylinder encounters an immobile sphere located at the central axis. The two 'slugs' located above and below the sphere in figures 9(*b*) and 10 are characterized by the sharp blue colour. There is a swirling flow that takes place above and below the sphere with opposite sense of rotation (figure 9*a*). This is discussed further below.

The exact form of a flow associated with Taylor columns induced by a solid body is a complicated problem depending on parameter regimes (Ekman, Reynolds and Rossby numbers) as well as the geometry (finite or infinite cylinder) of the body and ultimately its constitution (whether it is a solid or a liquid). Here, we will not pause to carry out a detailed enumeration of special cases arising in the various parameter regimes, geometries and materials; we will only point out certain qualitative similarities that exist between an odd viscous liquid and a rigidly rotating flow.

Figure 11 displays azimuthal and axial velocities of the liquid flowing in the cylinder of figures 9 and 10. Probes located at different elevations of the cylinder measure velocities as they vary in radial direction, from the cylinder central axis to its external surface, with a view to comparing our results to the experiments of Maxworthy (1970). In these numerical simulations, the Taylor and Maxworthy numbers are $\mathcal{T} = 50$ and $\mathcal{M} = 26$, respectively.

We find a velocity defect region (at $z = 70$ cm; cf. region I in the experiments of Maxworthy 1970), that is, the region where the velocity is less than that of the free stream. This is surrounded by the region $5 < r < 15$, which has a velocity in excess of that of

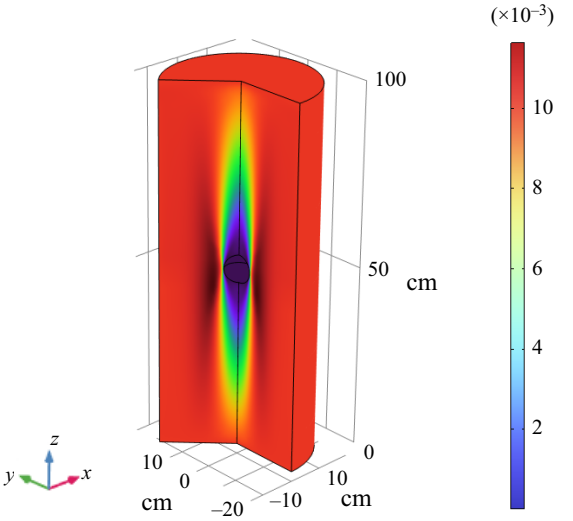

Figure 10. Three-dimensional realization of odd viscous flow around an immobile sphere (of radius 3.8 cm) located at elevation $z = 50$ in a moving cylinder with liquid entering from the top ($z = 100$ cm) and exiting at the bottom ($z = 0$), with the cylinder speed (the sphere is not allowed to rotate). The colour bar denotes the strength of the axial velocity w. A Taylor column of low axial velocity is visible circumscribing the sphere and surrounding the central axis. Parameters employed to produce this figure are odd viscosity coefficient $\eta_o = 0.5\,\mathrm{g\,(cm\,s)^{-1}}$, shear viscosity $\eta = 0.01\,\mathrm{g\,(cm\,s)^{-1}}$, cylinder radius 20 cm, sphere radius 3.8 cm, cylinder height $H = 100$ cm, liquid density $\rho = 1\,\mathrm{g\,cm^{-3}}$, and liquid velocity in the $-\hat{z}$ direction $U = 0.01\,\mathrm{cm\,s^{-1}}$. These give a Taylor number based on the sphere length scale $\mathcal{T} = 50$ and Maxworthy number $\mathcal{M} = 26.316$; see (6.2*a*,*b*).

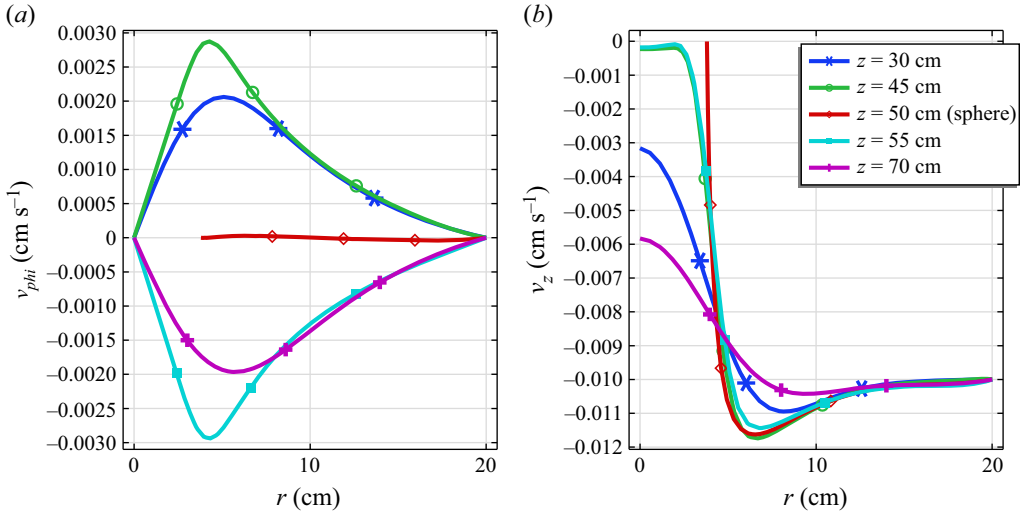

Figure 11. Plots of (*a*) azimuthal velocity v_ϕ and (*b*) axial velocity v_z, versus distance r from the central axis of the cylinder of figure 10, for an odd viscous liquid past a stationary sphere of radius 3.8 cm, located at elevation $z = 50$ cm. Each curve corresponds to a specific elevation in the cylinder where a probe has been placed. Two probes are located below the sphere at $z = 30$ and 45 cm, one lies at the level of the sphere ($z = 50$ cm), and two are located above the sphere at $z = 55$ and 70 cm. Plot (*a*) shows the counter-rotating azimuthal velocity components above and below the sphere, as was also depicted in figure 9(*a*). The magnitude of the azimuthal velocity decreases as one approaches the cylinder lids (at $z = 0$ and 100 cm) because liquid entering or leaving the cylinder has been set to have a vanishing azimuthal velocity component. The axial velocity of the liquid in (*b*) shows similarities (and differences) with respect to the analogous flow of a fluid in a rotating cylinder, as was described clearly by Maxworthy (1970, figure 7).

the free stream (region V in the experiments of Maxworthy 1970). The flow at $z = 30\,\text{cm}$ is narrower and has larger axial velocity than its mirror counterpart (at $z = 70\,\text{cm}$). Its angular velocity seems to be of the same magnitude compared with its mirror image (and this differs from the flow character in region VII of Maxworthy 1970).

The probe at $z = 55\,\text{cm}$ has a zero axial velocity close to the axis as this is determined by the Taylor–Proudman theorem, that the axial velocity of the slug is the same as the velocity of the body. The swirl, however, is non-zero and is actually quite large. This is region II in the experiments of Maxworthy (1970). An Ekman layer induces a slow axial velocity where the surface of the sphere meets the anisotropy axis (close to the $z = 45\,\text{cm}$ probe, and near $r = 0$). A sharp Ekman boundary layer is seen to form at $z = 50\,\text{cm}$, $r \sim 4\,\text{cm}$.

We have not observed an oscillatory region downstream of the sphere (region III of Maxworthy 1970), and we have not determined whether a region of clear fluid exists downstream and adjacent to the anisotropy axis.

Figures 9(*a*) and 11(*a*) show the counter-rotating character of the flow above and below the sphere, similar to figure 1 of Moore & Saffman (1968). The above discussion displays an indirect verification for the validity of the Taylor–Proudman theorem in the case of odd viscous flow with a velocity field (v_r, v_ϕ, v_z), where v_z has the velocity of the body ($v_z = 0$), v_r is virtually zero, and the flow outside the column is independent of z.

7. Vortex stretching and vortex twisting in a three-dimensional odd viscous liquid

The constitutive law (2.3) can be written in Cartesian coordinates in the form

$$\boldsymbol{\sigma}' = \eta_o \begin{pmatrix} -(\partial_x v + \partial_y u) & \partial_x u - \partial_y v & 0 \\ \partial_x u - \partial_y v & \partial_x v + \partial_y u & 0 \\ 0 & 0 & 0 \end{pmatrix}. \tag{7.1}$$

It is possible to define a modified pressure $\tilde{p} = p + \eta_o \zeta$, where $\zeta = \partial_x v - \partial_y u$ here is the component of vorticity in the z-direction. Then the odd Navier–Stokes equations are

$$\rho \frac{\mathrm{D}u}{\mathrm{D}t} = -\partial_x \tilde{p} + \eta_o\, \partial_y(\partial_z w), \quad \rho \frac{\mathrm{D}v}{\mathrm{D}t} = -\partial_y \tilde{p} - \eta_o\, \partial_x(\partial_z w), \quad \rho \frac{\mathrm{D}w}{\mathrm{D}t} = -\partial_z \tilde{p} + \eta_o\, \partial_z \zeta. \tag{7.2a–c}$$

What these equations show is that vortex stretching $\partial_z w$ will be important on a region in the x–y plane with vorticity ζ. To show this, let $\operatorname{curl} \boldsymbol{v} = (\xi, \eta, \zeta)$ be the components of vorticity in Cartesian coordinates, and consider a fluid particle whose vorticity points in the z-direction instantaneously (we perform this to simplify the nonlinear term $\operatorname{curl} \boldsymbol{v} \cdot \boldsymbol{\nabla} \boldsymbol{v}$ that arises in the vorticity equation (3.30)). Taking the curl of (7.2*a–c*), or considering directly the vorticity equation (3.30), we obtain

$$\frac{\mathrm{D}\xi}{\mathrm{D}t} = (\zeta - \eta_o \nabla_2^2)\, \partial_z u, \quad \frac{\mathrm{D}\eta}{\mathrm{D}t} = (\zeta - \eta_o \nabla_2^2)\, \partial_z v, \quad \frac{\mathrm{D}\zeta}{\mathrm{D}t} = (\zeta - \eta_o \nabla_2^2)\, \partial_z w. \tag{7.3a–c}$$

Thus the well-known vortex twisting, represented by the quantities $\partial_z u$ and $\partial_z v$ (cf. Tritton 1988, § 6.6), is now enhanced by the extra term $\eta_o(k_x^2 + k_y^2)$ appearing in the round brackets in (7.3*a–c*), induced by odd viscosity. Likewise, vortex stretching, represented by the quantity $\partial_z w$, is also enhanced by odd viscosity.

Of course, for a two-dimensional incompressible odd viscous liquid where the velocity does not depend on z, we have

$$\frac{\mathrm{D}\zeta}{\mathrm{D}t} = 0, \tag{7.4}$$

as is also known from the 'absorption' of the odd viscous force density into the pressure gradient see e.g. Ganeshan & Abanov 2017), thus the vorticity of a fluid particle in a two-dimensional odd viscous liquid is conserved.

8. The effect of both η_o and η_4 odd coefficients on fluid flow

Referring to the stress tensor (2.2), in this paper we assumed tacitly that only the coefficient η_3 was non-vanishing, which led the odd stress tensor to acquire the form (7.1) in Cartesian coordinates. The coefficient η_4 in (2.2) gives rise, however, to an additional odd stress tensor. In this section, we discuss the consequences of the latter, in the context of the effects developed in this paper.

As in § 2, we consider the field $\boldsymbol{b}$ to lie in the z-direction. Then the odd stress tensor acquires the additional components

$$\boldsymbol{\sigma}' = \eta_4 \begin{pmatrix} 0 & 0 & -(\partial_y w + \partial_z v) \\ 0 & 0 & \partial_x w + \partial_z u \\ -(\partial_y w + \partial_z v) & \partial_x w + \partial_z u & 0 \end{pmatrix}, \tag{8.1}$$

where we adopted the opposite sign to Lifshitz & Pitaevskii (1981, equation (58.16)). We proceed below to examine the form of inertial-like waves in an odd viscous liquid whose constitutive law is the combination of (7.1) and (8.1).

8.1. *Plane-polarized waves*

We define the linear operator

$$\mathcal{S} = (\nu_o - \nu_4)\, \nabla_2^2 + \nu_4\, \partial_z^2, \tag{8.2}$$

where $\nu_4 = \eta_4/\rho$, and $\nabla_2^2 = \partial_x^2 + \partial_y^2$. To obtain an understanding of the effect of odd viscosity parameters on the type of solutions, we classify the operator $\mathcal{S}$ in (8.2) as follows (assume here that $\nu_4 > 0$):

(i) $\mathcal{S}$ is elliptic when $\nu_o > \nu_4$;
(ii) $\mathcal{S}$ is hyperbolic when $\nu_o < \nu_4$;
(iii) $\mathcal{S}$ is parabolic when $\nu_o = \nu_4$.

Here, we have assumed that z plays the role of the time-like variable. This is the standard route followed in rigidly rotating liquids; see Whitham (1974, § 12.6). With the notation $\zeta = \partial_x v - \partial_y u$ for the component of vorticity in the z-direction, and a modified pressure $\tilde{p} = p + \eta_4 \zeta$, the Navier–Stokes equations (3.29) are replaced by

$$\frac{\mathrm{D}\boldsymbol{v}}{\mathrm{D}t} = -\frac{1}{\rho}\nabla\tilde{p} + \mathcal{S}\hat{\boldsymbol{z}} \times \boldsymbol{v}, \tag{8.3}$$

and the vorticity equation (3.31) by

$$\partial_t \operatorname{curl} \boldsymbol{v} = -\mathcal{S}\frac{\partial \boldsymbol{v}}{\partial z}. \tag{8.4}$$

With $\boldsymbol{v} = \boldsymbol{A}\exp(\mathrm{i}(\boldsymbol{k}\cdot\boldsymbol{r} - \omega t))$, the vorticity equation (8.4) becomes a system of three equations for the three unknown components of the amplitude $\boldsymbol{A}$. This system has a

non-trivial solution when the determinant of the matrix

$$\begin{pmatrix} -\mathrm{i}k_z\,\mathcal{S}(\boldsymbol{k}) & \omega k_z & -\omega k_y \\ -\omega k_z & -\mathrm{i}k_z\,\mathcal{S}(\boldsymbol{k}) & \omega k_x \\ \omega k_y & -\omega k_x & -\mathrm{i}k_z\,\mathcal{S}(\boldsymbol{k}) \end{pmatrix} \tag{8.5}$$

vanishes. Here,

$$\mathcal{S}(\boldsymbol{k}) = -(\nu_o - \nu_4)(k_x^2 + k_y^2) - \nu_4 k_z^2. \tag{8.6}$$

The dispersion relation becomes

$$\omega = \mp\mathcal{S}(\boldsymbol{k})\,\frac{k_z}{k} \quad \text{or} \quad \omega = \pm\cos(\theta)\,k^2\left[\nu_o - \nu_4 - (\nu_o - 2\nu_4)\cos^2\theta\right]. \tag{8.7}$$

Here and below, the reader can keep in mind the parabolic case $\nu_o = \nu_4$ and the elliptic case $\nu_o = 2\nu_4$ (parabolic and elliptic with respect to the operator $\mathcal{S}$ in (8.2)), which simplify all relations significantly and are to be discussed in what follows.

We display the dispersion (8.7) for $\nu_o = 0$ in figure 12(*a*), to be compared with figure 7. This dispersion relation is interesting as it crosses the $\omega = 0$ axis at angle $\theta = \pi/4$ (different to the $\pi/2$ of rigidly rotating liquids or the η_o of odd viscous liquid). Likewise, it has an inflection point at $\theta \neq \pi/2$, which signals the presence of a maximum for the group velocity that differs from those of rigidly rotating liquids and the η_o of odd viscous liquid. The group velocity (3.39*a*,*b*) is replaced by

$$\left(\frac{\partial\omega}{\partial k_x}, \frac{\partial\omega}{\partial k_y}\right) = \pm k\left((\nu_o - 2\nu_4)\cos^2\theta + \nu_o - \nu_4\right)\sin\theta\cos\theta\,(\cos\phi, \sin\phi), \tag{8.8}$$

$$\frac{\partial\omega}{\partial k_z} = \pm k\left((\nu_o - 2\nu_4)\cos^4\theta + (-2\nu_o + 5\nu_4)\cos^2\theta + \nu_o - \nu_4\right), \tag{8.9}$$

with modulus

$$|c_g| = k\Big[-5(\nu_o - 2\nu_4)^2\cos^6\theta + (7\nu_o - 16\nu_4)(\nu_o - 2\nu_4)\cos^4\theta - 3(\nu_o - \nu_4)(\nu_o - 3\nu_4)\cos^2\theta + (\nu_o - \nu_4)^2\Big]^{1/2}. \tag{8.10}$$

Its components and modulus are displayed in figure 12(*b*) for the case $\nu_o = 0$. The modulus of the group velocity displays a maximum at $\theta \neq \pi/2$, as expected from the properties of the corresponding dispersion relation (8.7).

When the flow field is determined by the plane-polarized waves $\boldsymbol{v} = \boldsymbol{A}\exp(\mathrm{i}(\boldsymbol{k}\cdot\boldsymbol{r} - \omega t))$ considered in this section, its helicity is conserved for an odd viscous liquid that incorporates both constitutive laws (7.1) and (8.1). That is the case because in wavenumber and frequency space, the linearized vorticity equation (8.4) can be written in the form

$$-\mathrm{i}\omega\boldsymbol{B} = -\mathrm{i}\boldsymbol{A}k_z\,\mathcal{S}(\boldsymbol{k}), \tag{8.11}$$

when $\operatorname{curl}\boldsymbol{v} = \boldsymbol{B}\exp(\mathrm{i}(\boldsymbol{k}\cdot\boldsymbol{r} - \omega t))$ and $\mathcal{S}(\boldsymbol{k})$ is defined in (8.6). Since $\omega = \mp\mathcal{S}(\boldsymbol{k})\,(k_z/k)$ (from (8.7)), we obtain $\boldsymbol{B} = \mp k\boldsymbol{A}$, or

$$\operatorname{curl}\boldsymbol{v} = \mp k\boldsymbol{v}. \tag{8.12}$$

Thus the helicity of the flow field determined by the odd stress tensors (7.1) and (8.1) is conserved:

$$\boldsymbol{v}\cdot\operatorname{curl}\boldsymbol{v} = \mp k\,|\boldsymbol{v}|^2. \tag{8.13}$$

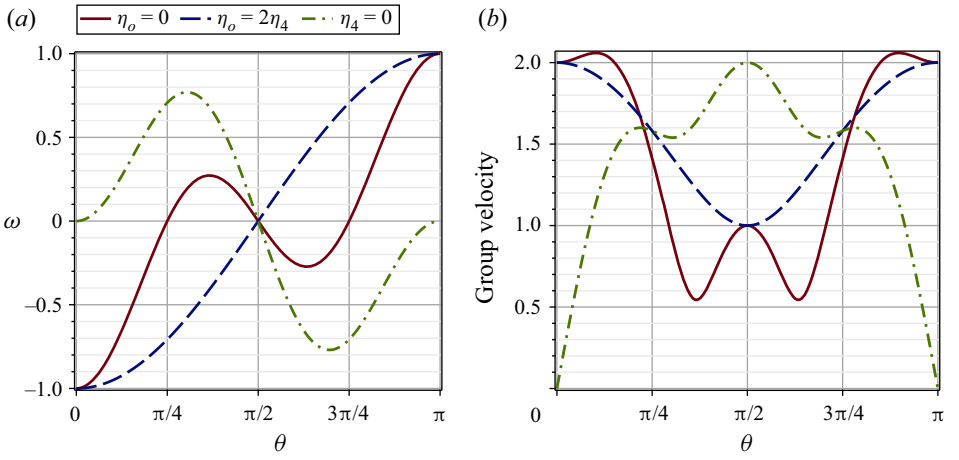

Figure 12. (*a*) Plane-polarized wave dispersion ω (see (8.7)) versus angle θ between the wavevector $\boldsymbol{k}$ and the z (anisotropy) axis (setting $k = -\nu_4 = 1$, $\nu_o = 0$). It differs qualitatively from its $\eta_o \neq 0$ counterpart displayed in figure 7 (and here denoted by the dash-dotted curve) by crossing the $\omega = 0$ axis at angles different from $\pi/2$. The case $\eta_0 = 2\eta_4$, discussed in detail in § 8.3, is denoted by the dashed curve. (*b*) Group velocity magnitude versus angle θ between the wavevector $\boldsymbol{k}$ and the z (anisotropy) axis, setting $k = -\nu_4 = 1$, $\nu_o = 0$. The magnitude develops maxima at angles $\theta \neq \pi/2$, differing from those of the rigidly rotating liquid or the η_o odd viscous liquid (here denoted by the dash-dotted curve); cf. figure 8. The case $\eta_0 = 2\eta_4$, discussed in detail in § 8.3, is denoted by the dashed curve.

In addition, $\boldsymbol{c}_g \cdot \boldsymbol{c}_p = 2[(\nu_o - 2\nu_4)\cos^2\theta - \nu_o + \nu_4]^2 k^2 \cos^2\theta = 2\,|\boldsymbol{c}_p|^2$, so the last two rows of table 1 remain unchanged.

Equation (8.3) can be employed to investigate the possibility of Taylor column formation in an odd viscous liquid that incorporates the stress tensor (7.1) and (8.1). Dropping the left-hand side of (8.3), it reads, in component form,

$$\frac{1}{\rho}\frac{\partial \tilde{p}}{\partial x} = -\mathcal{S}v, \quad \frac{1}{\rho}\frac{\partial \tilde{p}}{\partial y} = \mathcal{S}u, \quad \frac{\partial \tilde{p}}{\partial z} = 0, \tag{8.14a–c}$$

and carrying out the same manipulations as in § 5, we obtain the conditions

$$\partial_z \mathcal{S}u = \partial_z \mathcal{S}v = \partial_z \mathcal{S}w = 0 \quad \text{and} \quad \partial_x \mathcal{S}u + \partial_y \mathcal{S}v = 0, \tag{8.15a,b}$$

which replace (5.7). The forms of equations (8.14*a–c*) and (8.15*a*,*b*) are appealing and resemble (5.1*a–c*) and (5.7), respectively. They still lead to Taylor-column-like structures, which, however, are not identical to those of rigidly rotating liquids.

8.2. *Axisymmetric inertial-like waves when $\eta_o, \eta_4 \neq 0$*

We express the constitutive law (8.1) in cylindrical coordinates as

$$\boldsymbol{\sigma}' = \eta_4 \begin{pmatrix} 0 & 0 & -\left(\frac{1}{r}\partial_\phi v_z + \partial_z v_\phi\right) \\ 0 & 0 & \partial_r v_z + \partial_z v_r \\ -\left(\frac{1}{r}\partial_\phi v_z + \partial_z v_\phi\right) & \partial_r v_z + \partial_z v_r & 0 \end{pmatrix}, \tag{8.16}$$

and repeat the construction of axial waves of § 3.4. The linearized equations of motion (see Appendix A) become

$$-\mathrm{i}\omega v_r = -\frac{1}{\rho}\frac{\partial p'}{\partial r} - (\nu_o - \nu_4)\left[\frac{1}{r}\frac{\partial}{\partial r}\left(r\frac{\partial v_\phi}{\partial r}\right) - \frac{v_\phi}{r^2}\right] + \nu_4 k^2 v_\phi, \tag{8.17}$$

$$-\mathrm{i}\omega v_\phi = (\nu_o - \nu_4)\left[\frac{1}{r}\frac{\partial}{\partial r}\left(r\frac{\partial v_r}{\partial r}\right) - \frac{v_r}{r^2}\right] - \nu_4 k^2 v_r, \tag{8.18}$$

$$-\mathrm{i}\omega v_z = -\frac{\mathrm{i}k}{\rho}p' - \mathrm{i}k\nu_4\frac{1}{r}\frac{\partial}{\partial r}(r v_\phi), \tag{8.19}$$

where we simplified (8.18) by employing the incompressibility condition (3.4). Introducing the linear operator (3.8) $\mathcal{L} = \partial_r^2 + (1/r)\,\partial_r - 1/r^2$, the r and ϕ momentum equations become

$$-\mathrm{i}\omega v_r = -\mathrm{i}\frac{\omega}{k^2}\mathcal{L}v_r + \nu_4(\mathcal{L} + k^2)v_\phi - \nu_o\mathcal{L}v_\phi, \tag{8.20}$$

$$-\mathrm{i}\omega v_\phi = -\nu_4(\mathcal{L} + k^2)v_r + \nu_o\mathcal{L}v_r. \tag{8.21}$$

System (8.20)–(8.21) has a solution when the determinant $-(\nu_o - \nu_4)^2k^2\kappa^4 + (-2k^4\nu_o\nu_4 + 2k^4\nu_4^2 + \omega^2)\kappa^2 - k^2(k^2\nu_4 - \omega)(k^2\nu_4 + \omega)$ of the coefficients of the resulting linear system

$$\frac{\mathrm{i}Bk^4\nu_4 + \mathrm{i}(\nu_o - \nu_4)\kappa^2 Bk^2 - A\,\kappa^2\omega}{k^2\omega} - A = 0 \quad \text{and} \quad -\frac{\mathrm{i}A\left((\nu_o - \nu_4)\kappa^2 + k^2\nu_4\right)}{\omega} - B = 0 \tag{8.22a,b}$$

vanishes.

The velocity field is again expressed with respect to Bessel functions: $v_r = A\,\mathrm{J}_1(\kappa r)$ and $v_\phi = B\,\mathrm{J}_1(\kappa r)$. For real ω and k, the eigenvalue κ is

$$\kappa^2 = \frac{\pm\omega\sqrt{4(\nu_o - \nu_4)(\nu_o - 2\nu_4)k^4 + \omega^2} + \omega^2 - 2k^4\nu_4(\nu_o - \nu_4)}{2(\nu_o - \nu_4)^2k^2}. \tag{8.23}$$

To understand the structure of the solutions, we define the frequency squared parameter α and quartic power of frequency β of the form

$$\alpha = \omega^2 + 2k^4\nu_4(\nu_4 - \nu_o), \quad \beta = 4k^4(\nu_o - \nu_4)^2(\omega^2 - \nu_4^2k^4). \tag{8.24a,b}$$

With this notation, (8.23) simplifies to

$$2(\nu_o - \nu_4)^2k^2\kappa^2 = \alpha \pm \sqrt{\alpha^2 + \beta}. \tag{8.25}$$

In figure 13, we display all possible κ behaviours inherent in (8.23) and (8.25), and two cases are summarized in table 2. Thus, referring to figure 13, when $\eta_4 \equiv 0$, β is positive and there are two real and two imaginary roots κ (the case considered in § 3.4). When $\eta_o \equiv 0$, α is always positive and $\alpha^2 + \beta > 0$. Thus when $\beta < 0$, there are four real κ roots. In the opposite case, there are two imaginary and two real roots. In the elliptic case, $\eta_o = 2\eta_4$, there can be four imaginary or two imaginary and two real κ, as tabulated in table 2. The fact that the operator $\mathcal{S}$ in (8.2) is hyperbolic when $\nu_o = 0$, and elliptic when $\nu_o = 2\nu_4$, is reflected clearly in the type of roots κ and thus the form of the velocity field.

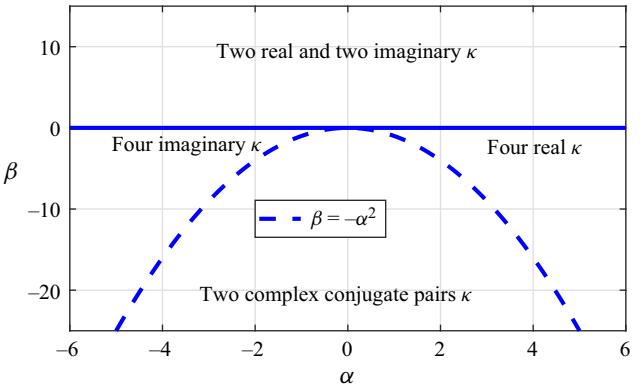

Figure 13. Behaviour of roots κ of (8.23) and (8.25) in the parameter space (α, β) defined in (8.24*a*,*b*). This includes the oscillatory Bessel functions for real κ, exponentially increasing/decreasing Bessel functions for imaginary κ, and exponential oscillating Bessel functions for complex κ.

		$\omega^2 < \nu_4^2 k^4$	$\nu_4^2 k^4 < \omega^2 < 2\nu_4^2 k^4$	$\omega^2 > 2\nu_4^2 k^4$
$\eta_o = 0$	α	+	+	+
	β	−	+	+
	κ	4 Re	2 Im + 2 Re	2 Im + 2 Re
$\eta_o = 2\eta_4$	α	−	−	+
	β	−	+	+
	κ	4 Im	2 Im + 2 Re	2 Im + 2 Re

Table 2. Types of roots κ from (8.23)/(8.25), where $\kappa^2 \propto \alpha \pm \sqrt{\alpha^2 + \beta}$ according to the sign of the parameters α and β defined in (8.24*a*,*b*) for two special choices of the odd viscosity parameters. In all cases, $\alpha^2 + \beta > 0$. Here, Re indicates real κ, and Im indicates imaginary κ.

Finally, of interest might also be the parabolic case where $\nu_o = \nu_4$. This case is separate from (8.23) since the equations determining κ are of second order in spatial derivatives (they are fourth order in the case (8.23)). We obtain

$$\kappa^2 = \frac{\left(k^4\nu_4^2 - \omega^2\right)k^2}{\omega^2}, \quad \omega = \pm\frac{\nu_4 k^3}{\sqrt{\kappa^2 + k^2}}, \tag{8.26a,b}$$

giving rise to either two real κ or two imaginary κ, and the dispersion relation.

8.3. *The $\eta_o = 2\eta_4$ case*

The governing differential operator $\mathcal{S}$ can be written in the form $(\nu_o - 2\nu_4)\,\nabla_2^2 + \nu_4\,\nabla^2$, thus in the limit $\nu_0 \to 2\nu_4$, $\mathcal{S}$ is just the Laplace operator

$$\mathcal{S} = \nu_4\,\nabla^2. \tag{8.27}$$

Mere inspection of the dispersion (8.7), group velocities (8.8)–(8.10) and parameter κ in (8.23), shows that they all contain the combination $\nu_o - 2\nu_4$. Setting this equal to zero makes the operator $\mathcal{S}$ elliptic, which has consequences for the direction of propagation of data along characteristics, in an odd viscous liquid. The dispersion relation (8.7),

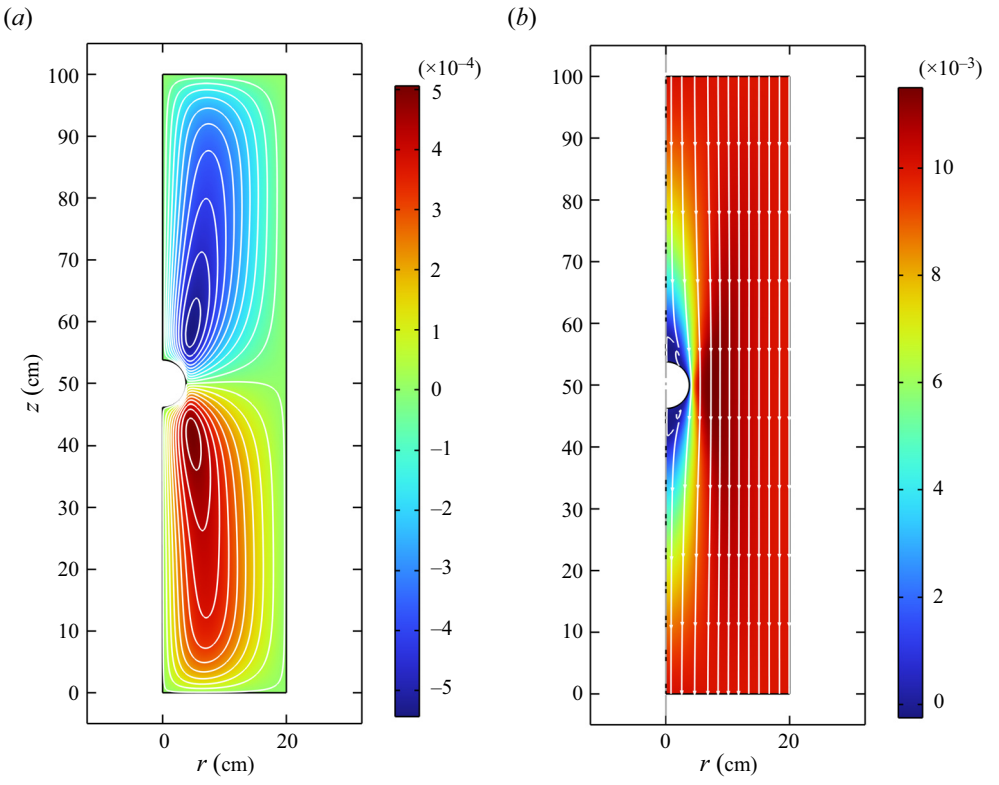

Figure 14. Distribution of (*a*) azimuthal and (*b*) axial velocity in an odd viscous liquid described by the constitutive laws (2.3) and (8.1) ($\eta_o = 2\eta_4 = 2\,\mathrm{g\,(cm\,s)^{-1}}$), moving slowly and meeting an immobile sphere (of radius 3.8 cm) located at elevation $z = 50$ cm at the centre axis of a cylinder. Liquid enters from the top ($z = 100$ cm) and exits at the bottom ($z = 0$). The sphere is not allowed to rotate. (*a*) Counter-rotation of liquid takes place above and below the sphere in the azimuthal direction, similar to figure 9. (*b*) A column whose generators are parallel to the cylinder axis and circumscribes the sphere is also visible, although its axial extent is smaller than that displayed in figure 9.

$\omega = -k^2((\nu_o - 2\nu_4)\cos^2\theta - \nu_o + \nu_4)\cos\theta$, simplifies significantly, giving

$$\omega = \nu_4 k k_z, \tag{8.28}$$

which recovers the dispersion relation of a Hamiltonian formulation of spinning molecules (Markovich & Lubensky 2021, equation (8)).

In addition, this combination was shown in a series of experiments of pressure-driven gas flow (Hulsman *et al.* 1970, equation (13)) to arise naturally in the limit of low magnetic field magnitude to pressure, $B/p \to 0$, as was also discussed by Khain *et al.* (2022). To this end, in table 2 we display the possible forms of roots κ obtained in (8.23) for the axisymmetric flow of the odd viscous liquid in a cylinder. Inertial oscillations (real κ) may be present, but they will be mixed with evanescent waves (imaginary κ), which will become prominent near the vessel walls.

In figure 12, we display the dispersion relation and group velocity of plane inertial-like waves for an odd viscous liquid with the combination $\eta_o = 2\eta_4$ (dashed curve). In addition, in figure 14, we repeat the simulations of figure 9 but for the combination $\eta_o = 2\eta_4$. The two figures are similar, which can be attributed to the fact that the governing differential operator $\mathcal{S}$ is elliptic in both cases. In figure 14(*b*), we observe that a Taylor-like

column is still present above and below the sphere located on the axis of the cylinder but its axial extent is reduced in comparison to figure 9(*b*). The distributions of azimuthal and axial velocities in the cylinder are very similar to those displayed in figure 11, and are not repeated here.

9. Discussion

In this paper, we showed that inertial-like waves and Taylor columns are generated in a three-dimensional odd viscous liquid. Both odd coefficients η_o and η_4 that appear in the constitutive laws (7.1) and (8.1) are nicely tucked away in a compact differential operator $\mathcal{S}$ (see (8.2)) and result in the odd form of the Navier–Stokes equations (8.3) and (8.4). The flow that arises from the consideration of plane-polarized waves is a Beltrami flow. Thus its helicity is conserved. The flow field determined by three-dimensional axisymmetric waves in an odd η_o and η_4 liquid has a structure that is determined by the eigenvalues κ in the argument of the Bessel function $\mathrm{J}_1(\kappa r)$ (or $\mathrm{Y}_1(\kappa r)$), and a classification of different behaviours is displayed in figure 13. Thus the velocity field can be oscillatory or exponential increasing/decaying, or a combination of these.

Considering the behaviour of liquids with a single η_o odd viscosity coefficient, we can isolate two important results that were developed here. First, we observe inertial oscillations downstream of a slowly moving body whose theoretically determined wavelength (3.25) is in agreement with its estimate from solutions of the full Navier–Stokes equations (in a manner analogous to the experiments of Long (1953), which were in agreement with the theory of inertial oscillations in rigidly rotating liquids; cf. Batchelor 1967, plate 24). Second, we observe Taylor-column-like behaviour when a sphere moves slowly along the axis of anisotropy, and this also resembles the behaviour of a rigidly-rotating liquid, for instance, in the experiments of Maxworthy (1970). The latter behaviour is to be expected since when the wavevector is perpendicular to the anisotropy axis, the flow becomes effectively two-dimensional in agreement with the (modified) Taylor–Proudman theorem that we developed here, suitable for odd viscous liquids. At the same time, helicity segregation signals the generation of inertial-like waves at the interior of the column, where information is transported along the anisotropy axis, above the body and below the body at the group velocity. Referring to existing experiments measuring the odd viscous coefficients η_o and η_4 in pressure-driven flow of polyatomic gases in the presence of a magnetic field B (cf. Hulsman *et al.* 1970), the combination $\eta_o = 2\eta_4$ becomes prominent in the limit of small ratio of magnetic field to pressure ($B/p \to 0$). We performed a dedicated discussion of this case in § 8.3, showing that all observables simplify significantly, and that the fluid flow behaviour is dominated by the character of the differential operator $\mathcal{S}$ defined in (8.2), which reduces to the Laplace operator.

Our theoretical discussion was centred predominantly on an odd viscous liquid with zero shear viscosity. (In the numerical simulations of the Navier–Stokes equations, shear viscosity was, however, small but non-zero.) Shear viscosity would just endow the frequency ω with an imaginary part, as is the case in rigidly rotating liquids; see, for instance, Chandrasekhar (1961, p. 86, equation (72)).

There is a large number of unexplored phenomena in three-dimensional odd viscous liquids associated with the findings in this paper. To name a few, consider the effects of: shear viscosity on Taylor columns, and thus the establishment of Ekman and Stewartson layers; different flow conditions (e.g. flow incident on a finite length obstacle also generating Taylor columns); different material properties (e.g. a liquid droplet instead of a

solid sphere rising slowly in such a liquid; cf. Bush *et al.* 1995; Bush, Stone & Bloxham 1995); a freely suspended sphere rising slowly in such a liquid; and finally, an experimental realization of these effects. Also consider determination of criteria for Taylor-column formation in bounded and unbounded domains. To understand the diversity behind these issues in the case of rotating liquids, see the review of Bush *et al.* (1995).

The formulation developed in this paper can prove to be useful in many areas of research. For instance, one could envision the following application of odd viscous liquid Taylor columns to materials science. Semiconducting nanowires, employed in diverse fields such as biological molecule sensing and living cell probing, are manufactured by the vapour–liquid–solid growth technique, whereby a liquid alloy droplet increases in size by absorbing material from a vapour phase. Hydrodynamics has been shown to be an important factor in this process (Schwalbach *et al.* 2012). Disruption of growth may take place in the form of instabilities leading the nanowire to adopt distorted shapes or to develop random extrusions. These instability mechanisms may, however, become suppressed in the presence of odd viscosity. Slow impinging flow on a nanowire will circumscribe each one of them to its own Taylor column, thus providing a unidirectional guide for droplet alloy growth, circumventing the generation of instabilities. Thus a fundamental related open question concerns the effect that odd viscosity has on convection.

Acknowledgements. We thank L. Lopez and four anonymous referees for comments that improved the manuscript.

Funding. This research was supported by the Center for Bio-Inspired Energy Science, an Energy Frontier Research Center funded by the US Department of Energy, Office of Science, Basic Energy Sciences under award no. DE-SC0000989.

Declaration of interests. The authors report no conflict of interest.

Author ORCIDs.
E. Kirkinis https://orcid.org/0000-0002-1140-9632;
M. Olvera de la Cruz https://orcid.org/0000-0002-9802-3627.

Appendix A. Linearized equations of motion

The linearized equations of motion are

$$\partial_t v_r = -\frac{1}{\rho}\frac{\partial p'}{\partial r} + \frac{1}{\rho}\left[\frac{1}{r}\,\partial_r(r\sigma_{rr}) + \frac{1}{r}\,\partial_\phi\sigma_{r\phi} + \partial_z\sigma_{rz} - \frac{1}{r}\,\sigma_{\phi\phi}\right], \tag{A1}$$

$$\partial_t v_\phi = -\frac{1}{\rho r}\frac{\partial p'}{\partial \phi} + \frac{1}{\rho}\left[\frac{1}{r^2}\,\partial_r(r^2\sigma_{\phi r}) + \frac{1}{r}\,\partial_\phi\sigma_{\phi\phi} + \partial_z\sigma_{\phi z} + \frac{1}{r}\,(\sigma_{r\phi} - \sigma_{\phi r})\right], \tag{A2}$$

$$\partial_t v_z = -\frac{1}{\rho}\frac{\partial p'}{\partial z} + \frac{1}{\rho}\left[\frac{1}{r}\,\partial_r(r\sigma_{zr}) + \frac{1}{r}\,\partial_\phi\sigma_{z\phi} + \partial_z\sigma_{zz}\right]. \tag{A3}$$

Note that the definition of the stress tensor in fluid mechanics (cf. Landau & Lifshitz 1987) differs from its definition in the continuum mechanics literature, where it is defined as the transpose. Here, we follow the fluid mechanics notation, as this arises, for instance, in Landau & Lifshitz (1987).

Appendix B. Basic facts about rotating fluids

The Rossby and Ekman numbers are

$$Ro = \frac{U}{\Omega L}, \quad E = \frac{\nu}{\Omega L^2}. \tag{B1a,b}$$

In the axisymmetric case where $\partial_\phi = 0$, the Taylor–Proudman theorem for the geostrophic equations

$$-\Omega v_\phi = -\frac{1}{\rho}\frac{\partial p}{\partial r}, \quad \Omega v_r = 0, \quad 0 = \frac{\partial p}{\partial r} \tag{B2a–c}$$

implies that $v_r \equiv 0$ and thus the streamlines are spirals that wound around circular cylinders (Yih 1959).

B.1. *Taylor columns*

The geostrophic equations, in Cartesian coordinates, written in the form

$$\frac{1}{\rho}\frac{\partial p}{\partial x} = -\Omega v, \quad \frac{1}{\rho}\frac{\partial p}{\partial y} = \Omega u, \quad \frac{\partial p}{\partial z} = 0, \tag{B3a–c}$$

show that the pressure p is a streamfunction and thus constant on a streamline of the flow. A finite-length cylinder with generators parallel to the rotating axis and moving horizontally in a rotating liquid will thus be accompanied by a liquid velocity parallel to its generators, and a column will accompany its motion (Yih 1988, § 12.2). Inside the column, the velocity can be zero, although viscous liquids are accompanied with special flows where the velocity does not vanish (Moore & Saffman 1968).

Separate two-dimensional flows exist inside and outside the Taylor column. Liquid cannot be transferred between these two regions. This is clear in the axisymmetric case where v_r vanishes everywhere (outside the Taylor column). Experimentally, dye that is outside the Taylor column cannot enter, and dye inside does not exit (Tritton 1988, figure 16.2). The flow inside the Taylor column is determined by taking into account the thin shear layers that develop on the lateral surface of the Taylor column and the Ekman boundary layers on the body and the boundaries (Moore & Saffman 1968).

B.2. *Elasticity induced by rotation of an inviscid liquid*

Consider a particle of unit mass that moves with speed v perpendicular to the axis of rotation. Momentum conservation gives

$$\frac{v^2}{r} = 2\Omega v. \tag{B4}$$

Solving for r, we obtain $r = v/2\Omega$. This implies that the locus of the particle is a circle. It goes around the circle twice during every revolution of the liquid with period $T = 2\pi r/v = \pi/\Omega$ (the vorticity of the liquid in rigid-body rotation is twice the angular velocity of rotation) (Tritton 1988, § 16.6).

The effect of this constraining tendency is to support inertial waves. As remarked above, inertial waves exist only when $\omega < 2\Omega$ since $\kappa = k\sqrt{4\Omega^2/\omega^2 - 1}$ must be real.

The relations (Taylor–Proudman theorem)

$$\frac{\partial u}{\partial z} = \frac{\partial v}{\partial z} = 0 \tag{B5}$$

do not allow vortex twisting (the liquid velocity approaching a finite obstacle does not change relative to the obstacle – vorticity is not generated); see (Tritton 1988, figure 16.5). This means that the background vorticity resists twisting. On the other hand, the condition

$$\frac{\partial w}{\partial z} = 0 \tag{B6}$$

resists vortex stretching (vortex tubes do not thin to increase vorticity; see Tritton 1988, figure 16.6).

Another view of the same effect is to displace a circular ring of fluid outwards to a new position r. The circulation $2\pi vr$ along that ring remains the same according to Kelvin's theorem. Thus, the liquid velocity v and scaled inertial force v^2/r will be smaller in the new position. Prior to the displacement, the scaled inertial force v^2/r was larger at position r, and it was balanced exactly by a pressure gradient, which now sees the lower v^2/r of the ring. Thus it will push the ring back towards its original position. The pressure at this position will push it again outwards, and the ring will experience an oscillatory motion (Yih 1988, § 5). See also Davidson (2013, chap. 1) for a more detailed explanation of the same effect. A similar discussion about the restoring effect of the Coriolis force can be traced back to Batchelor (1967, § 7.6).

References

Abanov, A., Can, T. & Ganeshan, S. 2018 Odd surface waves in two-dimensional incompressible fluids. *SciPost Phys.* **5** (1), 010.

Asselin, O. & Young, W.R. 2020 Penetration of wind-generated near-inertial waves into a turbulent ocean. *J. Phys. Oceanogr.* **50** (6), 1699–1716.

Avron, J.E. 1998 Odd viscosity. *J. Stat. Phys.* **92** (3–4), 543–557.

Avron, J.E., Seiler, R. & Zograf, P.G. 1995 Viscosity of quantum Hall fluids. *Phys. Rev. Lett.* **75** (4), 697.

Banerjee, D., Souslov, A., Abanov, A.G. & Vitelli, V. 2017 Odd viscosity in chiral active fluids. *Nat. Commun.* **8** (1), 1573.

Batchelor, G.K. 1967 *An Introduction to Fluid Dynamics*. Cambridge University Press.

Bire, S., Kang, W., Ramadhan, A., Campin, J.-M. & Marshall, J. 2022 Exploring ocean circulation on icy moons heated from below. *J. Geophys. Res.* **127**, e2021JE007025.

Bush, J.W.M., Stone, H.A. & Bloxham, J. 1995 Axial drop motion in rotating fluids. *J. Fluid Mech.* **282**, 247–278.

Bush, J.W.M., Stone, H.A. & Tanzosh, J.P. 1995 Particle motion in rotating viscous fluids: historical survey and recent developments. *Curr. Top. Phys. Fluids* **1**, 337–355.

Chandrasekhar, S. 1961 *Hydrodynamic and Hydromagnetic Stability*. Oxford University Press.

Dahler, J.S. & Scriven, L.E. 1961 Angular momentum of continua. *Nature* **192**, 36–37.

Davidson, P.A. 2013 *Turbulence in Rotating, Stratified and Electrically Conducting Fluids*. Cambridge University Press.

Davidson, P.A. 2014 The dynamics and scaling laws of planetary dynamos driven by inertial waves. *Geophys. J. Intl* **198** (3), 1832–1847.

Davidson, P.A. & Ranjan, A. 2018 On the spatial segregation of helicity by inertial waves in dynamo simulations and planetary cores. *J. Fluid Mech.* **851**, 268–287.

Dransfeld, L., Dwane, O. & Zuur, A.F. 2009 Distribution patterns of ichthyoplankton communities in different ecosystems of the Northeast Atlantic. *Fish. Oceanogr.* **18** (6), 470–475.

Fruchart, M., Scheibner, C. & Vitelli, V. 2023 Odd viscosity and odd elasticity. *Annu. Rev. Condens. Matter Phys.* **14**, 471–510.

Ganeshan, S. & Abanov, A.G. 2017 Odd viscosity in two-dimensional incompressible fluids. *Phys. Rev. Fluids* **2** (9), 094101.

GAO, F., CHEW, J.W. & MARXEN, O. 2020 Inertial waves in turbine rim seal flows. *Phys. Rev. Fluids* **5** (2), 024802.

GREENSPAN, H.P. 1968 *The Theory of Rotating Fluids*. Cambridge University Press.

HULSMAN, H., VAN WAASDIJK, E.J., BURGMANS, A.L.J., KNAAP, H.F.P. & BEENAKKER, J.J.M. 1970 Transverse momentum transport in polyatomic gases under the influence of a magnetic field. *Physica* **50** (1), 53–76.

KHAIN, T., SCHEIBNER, C., FRUCHART, M. & VITELLI, V. 2022 Stokes flows in three-dimensional fluids with odd and parity-violating viscosities. *J. Fluid Mech.* **934**, A23.

KIRKINIS, E. 2017 Magnetic torque-induced suppression of van-der-Waals-driven thin liquid film rupture. *J. Fluid Mech.* **813**, 991–1006.

KIRKINIS, E. 2023 Null-divergence nature of the odd viscous stress for an incompressible liquid. *Phys. Rev. Fluids* **8** (1), 014104.

KIRKINIS, E. & ANDREEV, A.V. 2019 Odd viscosity-induced stabilization of viscous thin liquid films. *J. Fluid Mech.* **878**, 169–189.

LANDAU, L.D. & LIFSHITZ, E.M. 1987 *Fluid Mechanics*, vol. 6. Course of Theoretical Physics. Pergamon Press Ltd.

LIFSHITZ, E.M. & PITAEVSKII, L.P. 1981 *Physical Kinetics*, vol. 10. Course of Theoretical Physics. Pergamon Press.

LONG, R.R. 1953 Steady motion around a symmetrical obstacle moving along the axis of a rotating liquid. *J. Atmos. Sci.* **10** (3), 197–203.

MARKOVICH, T. & LUBENSKY, T.C. 2021 Odd viscosity in active matter: microscopic origin and 3D effects. *Phys. Rev. Lett.* **127** (4), 048001.

MAXWORTHY, T. 1970 The flow created by a sphere moving along the axis of a rotating, slightly-viscous fluid. *J. Fluid Mech.* **40** (3), 453–479.

MOFFATT, H.K. 1969 The degree of knottedness of tangled vortex lines. *J. Fluid Mech.* **35** (1), 117–129.

MOFFATT, H.K. 1970 Dynamo action associated with random inertial waves in a rotating conducting fluid. *J. Fluid Mech.* **44** (4), 705–719.

MOORE, D.W. & SAFFMAN, P.G. 1968 The rise of a body through a rotating fluid in a container of finite length. *J. Fluid Mech.* **31** (4), 635–642.

OGILVIE, G.I. 2013 Tides in rotating barotropic fluid bodies: the contribution of inertial waves and the role of internal structure. *Mon. Not. R. Astron. Soc.* **429** (1), 613–632.

RINALDI, C. 2002 Continuum modeling of polarizable systems. PhD thesis, Massachusetts Institute of Technology.

SCHWALBACH, E.J., DAVIS, S.H., VOORHEES, P.W., WARREN, J.A. & WHEELER, D. 2012 Stability and topological transformations of liquid droplets on vapor–liquid–solid nanowires. *J. Appl. Phys.* **111** (2), 024302.

SONI, V., BILILIGN, E.S., MAGKIRIADOU, S., SACANNA, S., BARTOLO, D., SHELLEY, M.J. & IRVINE, W.T.M. 2019 The odd free surface flows of a colloidal chiral fluid. *Nat. Phys.* **15** (11), 1188–1194.

TANZOSH, J.P. & STONE, H.A. 1994 Motion of a rigid particle in a rotating viscous flow: an integral equation approach. *J. Fluid Mech.* **275**, 225–256.

TRITTON, D.J. 1988 *Physical Fluid Dynamics*. Oxford University Press.

TRUESDELL, C. & NOLL, W. 1992 *The Nonlinear Field Theories Of Mechanics*, 2nd edn. Springer.

WHITHAM, G.B. 1974 *Linear and Nonlinear Waves*. Wiley.

YIH, C.-S. 1959 Effects of gravitational or electromagnetic fields on fluid motion. *Q. Appl. Maths* **16** (4), 409–415.

YIH, C.-S. 1988 *Fluid Mechanics*. West River Press.